THE EFFICACY OF BISPHOSPHONATE PRE-TREATMENT IN PREVENTING LOSSES IN DENSITOMETRIC AND MECHANICAL PROPERTIES DURING HINDLIMB UNLOADING AND THROUGHOUT REAMBULATION IN THE DISTAL FEMUR METAPHYSIS OF ADULT MALE RATS

A Thesis

by

JENNIFER LAUREN KOSNIEWSKI

Submitted to the Office of Graduate and Professional Studies of
Texas A&M University
in partial fulfillment of the requirements for the degree of

MASTER OF SCIENCE

Chair of Committee,	Harry A. Hogan
Committee Members,	Susan A. Bloomfield
	Seok Chang Ryu
Head of Department,	Andreas Polycarpou

May 2017

Major Subject: Mechanical Engineering

ABSTRACT

Microgravity-related bone loss in astronauts is a well-known consequence of space travel. These losses are a result of the catabolic reaction of the skeleton to unloading. Anti-catabolics like bisphosphonates (BPs) have been used to combat bone loss in osteoporosis patients. Their mechanism of action also makes them a possible treatment for preventing the microgravity induced bone loss experienced by astronauts. There are a variety of BPs on the market, and many choices in treatment administration schedule. In this study, the efficacy of pre-treatment with BPs was evaluated by observing changes in bone densitometry measures, geometry, and mechanical properties over different periods. The periods of interest were the hindlimb unloading (HU) period during which microgravity is simulated and the recovery period following HU.

Simulating microgravity is achieved by hindlimb unloading adult rats using the model described by Morey-Holton. Six-month old Sprague-Dawley rats were split into four groups which were ambulatory controls (AC), hindlimb unloading controls (HUC), risedronate pre-treatment (RIS), alendronate pre-treatment (ALN). During the 28 day pre-treatment period, the ALN and RIS groups were administered their respective BP pre-treatments. Following that, all groups except the ambulatory controls underwent a 28 day unloading period. Rats were reambulated and recovered for 56 days after the unloading period. Bones were harvested at baseline (day 0), end of pre-treatment (day 28), end of unloading (day 56), end of recovery (day 112) and analyzed. *Ex vivo* scans of the distal femur metaphysis (DFM) were taken using both peripheral quantitative computed tomography (pQCT) and micro computed tomography (μCT). Cross-section specimens of the DFM were isolated and compressed between two platens to estimate mechanical properties. The results of scans and tests were analyzed to determine if the pre-treatment approach prevented bone loss during HU and throughout recovery. A BP was considered protective if there were significant differences between the HUC group and AC group, but no difference between the AC group and the respective BP group.

The resulting data demonstrated that both pre-treatments prevented (HU) related losses that the HUC group experienced in several densitometric and geometric parameters. HUC did not see statistically significant losses in mechanical properties; however, RIS did enhance them as compared to HUC after HU. The AC group experienced losses in cancellous bone at the end of recovery which were likely attributable to age-related decline. When AC was lowest, either both treatment groups or just RIS were significantly better. Both BP groups had enhanced intrinsic mechanical properties at the end of recovery as compared to AC. It was a reoccurring trend that RIS was significantly better than HUC while ALN would differ from neither HUC nor AC. This was true for all mechanical properties, trabecular number, and trabecular spacing after HU. After recovery, the control group (HUC or AC) with the lowest average value varied so this trend in indirect BP group differences becomes less clear. The RIS group had the lowest average densitometric and geometric results in the cortical region.

Risedronate seemed to have the stronger effect on cancellous bone and total bone over the unloading period. However, the RIS group's protection of the cortical region seemed to dissipate by the end of recovery. ALN was only slightly inferior to RIS and still protected bone during HU. Alendronate's beneficial effects also seemed to persist better than RIS' effects did through the recovery period in both the cortical and cancellous regions. Risedronate was the more effective BP while it persisted, but this was at the cost of inferior retention in the cortical region during recovery.

These results suggest that pre-treatment with either BP would be effective at combatting bone loss due to mechanical unloading. Comparisons with the results of other studies, though limited by differences in design, indicate that a pre-treatment approach is as effective in protecting bone as concurrent treatment. In some cases, it appears that the pre-treatment approach may be more effective. Their enhancement of mechanical performance makes BP pre-treatment a promising course of treatment for astronauts. Practical limitations would likely necessitate this BP pre-treatment approach to be tested in combination with aRED in a human spaceflight study. However, this pre-treatment approach could first be assessed with a controlled human bedrest study.

ACKNOWLEDGEMENTS

I would like to thank my two committee members for their time and contributions. Specifically I would like to thank Dr. Ryu for asking many questions of "Why?" which helped remind me to explain and justify details of the study. In addition, I would like to thank Dr. Bloomfield being a collaborator on this study as well as a committee member. I appreciate her willingness to explain the more physiological side of things throughout my time in the Bone Biomechanics Lab. I would like to give special thanks to Dr. Hogan for being both my committee chair and the type of PI who brings treats to lab meetings. His guidance has helped me grow to understand a great deal about bone biomechanics without taking any BMEN classes and our discussions on statistics are always engaging.

The data presented in this thesis are only a small part of a much larger study that numerous people have helped to make possible. Funding was provided by NASA grant #NNX13AM43G. In the first half of this large study, there were over 130 animals split into 3 cohorts. The animal work and bone harvesting was a collaborative effort between the undergraduate and graduate students in the Bone Biomechanics lab and the Bone Biology lab of Dr. Bloomfield (Department of Health and Kinesiology, Texas A&M University). Without this collaboration between everyone, animal work would have been nigh impossible to complete in a timely manner or maybe at all. Micro CT scanning would not have been possible without Dr. Larry Suva (Professor and Head, Department of Veterinary Physiology & Pharmacology, Texas A&M University) who oversaw the scanning of our specimens. All RPC testing required at least two people at a time and Jeremy Black and JP Elizondo graciously alternated being the second person.

Finally, I would like to thank my parents Maggie and Tom, sister Katie, brother-in-law David and my friends Rex and Rob for their support through the process. When I got discouraged or tired they would always be there to tell me to keep going.

CONTRIBUTORS AND FUNDING SOURCES

Contributors

This work was supervised by a thesis committee consisting of Professor Harry Hogan and Professor Seok Chang Ryu of the Department of Mechanical Engineering and Professor Susan Bloomfield of the Department of Health and Kinesiology.

The data analyzed in Section 4.1.2 was provided by Professor Larry Suva (Professor and Head, Department of Veterinary Physiology & Pharmacology, Texas A&M University) whose students were responsible for the scanning and the post-processing. Statistical analysis of the data was performed by the student.

Scan data from Section 4.1.1 was collected by a coworker in the same lab, Jon Paul Elizondo, but was processed and analyzed by the student.

Preparation and testing of samples for Section 4.2 was done in collaboration with lab coworkers Jeremy Black and Jon Paul Elizondo. Calculations, processing, and analysis were done by the student.

All other work conducted for the thesis was completed by the student independently.

Funding Sources

This work was made possible in part by NASA under Grant Number NNX13AM43G.

NOMENCLATURE

vBMD	Volumetric Bone Mineral Density
BMC	Bone Mineral Content
BV/TV	Bone Volume per Total Volume
DA	Degree of Anisotropy
μCT	Micro Computed Tomography
PBS	Phosphate Buffered Saline
pQCT	Peripheral Quantitative Computed Tomography
ROI	Region of Interest
Tb.Th	Trabecular Thickness
Tb.N	Trabecular Number
Tb.Sp	Trabecular Spacing

TABLE OF CONTENTS

Page

LIST OF FIGURES

Page

Page

LIST OF TABLES

Page

1. INTRODUCTION

One of the major issues that continues to face astronauts going to space is the effect microgravity has on their skeleton. Studies have shown that bone loss in space varies by site. Important mixed bone sites like the spine, femoral neck, and trochanter can experience losses of between 1 and 1.5% BMD (bone mineral density) per month when countermeasures are not taken [2]. This is a large loss for a single month of mechanical unloading considering female post-menopausal osteoporosis sufferers generally lose between 0.86 and 1.12% BMD per year at these sites [3]. High monthly losses in BMD pose a problem for long term space travel given that typical ISS (International Space Station) missions are 4-6 months in duration and a Mars mission will last 1-3 years.

The current countermeasure to bone loss in astronauts is exercise using the advanced resistance exercise device (aRED). Studies have found that using the device mostly protects bone, but that there are still losses at the hip and femoral neck [4]. Additionally, bone resorption marker levels were still high in exercisers. Combining aRED exercise with osteoporosis drug (bisphosphonate) treatment suppressed resorption and prevented these losses [5]. Those findings are the sole study using bisphosphonates (BPs) in astronauts and did not include a non-exercising BP-treated group. Studying the effects of BPs alone is thus important since they have demonstrated potential when combined with exercise. There is also a concern with aRED's feasibility for long duration flights where its weight would pose a problem. Greater weight requires different capsule configuration and increases the cost of the launch.

Little is known about the actual mechanical integrity of bone in human studies of microgravity's effects. Strength indices and fracture risks estimated in those studies are based on computed tomography (CT) data, which quantifies densitometry and geometry [4]. The problem with this approach is that osteoporosis studies have found that a large portion (>50%) of low trauma fractures occur in those whose BMD values are above those defined as osteoporotic [6][7]. Assessing strength and fracture risk with CT data

alone is insufficient to characterize expected mechanical performance in astronauts. Destructive and nondestructive mechanical testing will be needed to get a more accurate measure of microgravity's effect on biomechanics. This justifies the need for using relevant animal models.

The skeleton responds to the loading it regularly experiences by modeling and remodeling bone to suit those loads [8]. Both processes involve resorption of bone by cells called osteoclasts and formation of new bone by cells called osteoblasts. In modeling, resorption and formation occur at different sites and is the process for skeletal growth and shaping through maturation. During remodeling, resorption and formation occur at the same, or close, sites to either repair or better suit loading. Increased or imbalanced resorption occurs both in osteoporosis sufferers and in astronauts during spaceflight. In astronauts, this increase is due to the sharply reduced gravitational loading in space.

The two main approaches to combatting bone loss are anti-catabolic and anabolic. Anti-catabolic approaches aim to arrest the resorption of bone while anabolics promote formation. Anti-catabolic treatments, specifically bisphosphonate (BP) drugs, are already widely used to treat post-menopausal osteoporosis [9]. Some bisphosphonates cause osteoclasts to undergo apoptosis and die which in turn reduces resorption. However, many modern BPs simply deactivate osteoclasts to reduce resorption. The most popular approach for attenuating bone loss in astronauts is an anabolic resistance exercise approach using the aRED [10]. Studies have also shown promising results for a combination of exercise and strict dietary and nutritional guidelines [11]. As noted previously, there has been only one study of BP-supplemented exercise and treatment was administered inflight. Results indicated that a BP supplement to exercise attenuated the losses at the hip and femoral neck that exercise alone did not [5].

Animal models of simulated microgravity are useful tools for studying the effects of unloading on the musculoskeletal system more comprehensively. These models allow for careful control of experimental variables which is not feasible during spaceflight

missions. They also are advantageous in that destructive mechanical testing can be performed on harvested bones and bone tissue. Mechanical tests performed could be bending of the long bones, offset loading of the femoral head, compression of cancellous bone, or other tests as appropriate. This testing would help satisfy the need for accurate mechanical characterization rather than relying on estimates derived from CT data. As noted previously, estimations based on CT data tend to be poor indications of fracture risk [6][7]. Actual spaceflight studies have examined BP treatment only when combined with aRED exercise. This is understandable and the only plausible scenario for actual spaceflight studies, given the wide range of benefits from regular exercise. Thus, an animal model also has the advantage of being usable to examine the performance of BPs separately to determine their unique contributions and effects.

This thesis study is part of a larger research project funded by a National Aeronautics and Space Administration (NASA) Space Biology grant (number #NNX13AM43G). In this broader project, four different pre-treatments are being examined. The BP pre-treatments are the two anti-catabolic pre-treatments and the other two pre-treatment are anabolic (one pharmacologic and one exercise based). In all cases, treatments are administered to rats (over a 28 day period) prior to exposing them to simulated microgravity using the hindlimb unloading (HU) rat model. This thesis includes only the BP pre-treatments, as the anabolic pre-treatment half of the study is ongoing. Six month old Sprague-Dawley rats are the standard animal model for the lab. At six months old, these rats are considered skeletally mature. The pre-treatment period which lasts 28 days is followed by 28 days of HU and then 56 days of reambulation recovery. Various bones were collected at key time points, but the scope of this thesis is limited to the distal femur metaphysis (DFM) which is shown in Figure 1.

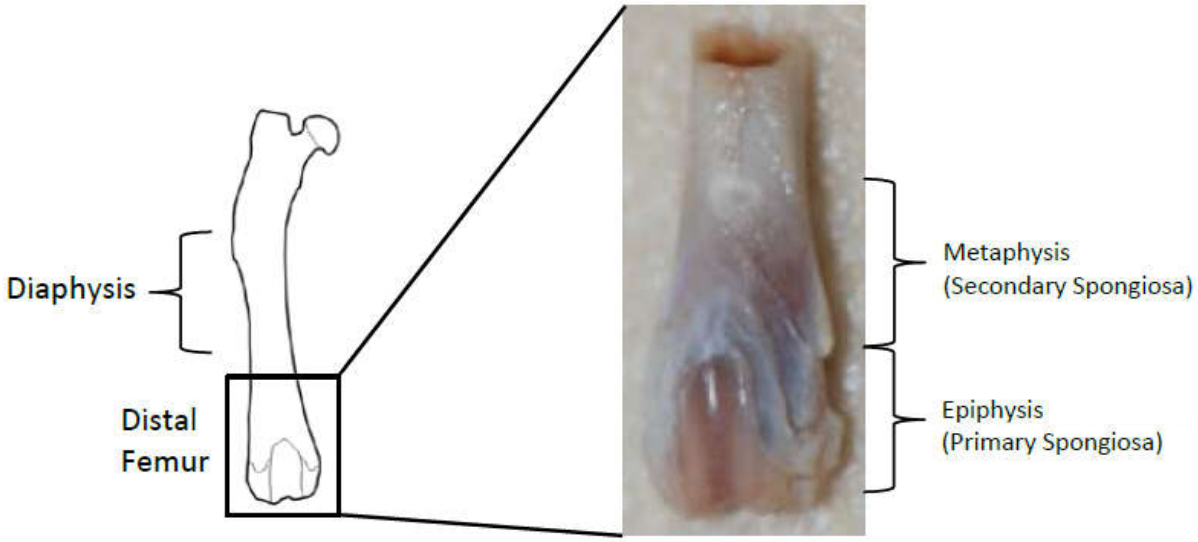

Figure 1: Diagram of Whole Femur with Distal Region and Distal Metaphysis Indicated

This site was chosen because it is a mixed bone site composed of both cortical and cancellous bone. In this regard, it is similar to the femoral neck in humans. While rat femoral necks have both cortical and cancellous bone, the proportion of cortical to cancellous tissue differs substantially from that in humans [12]. The distal femur metaphysis was used as its cancellous-to-cortical proportion is more similar to the human femoral neck.

A specific topic of interest for this study is whether administration of BPs as a pre-treatment rather than concurrent with unloading would be effective or not. If shown to be effective, then adopting a pre-treatment approach for astronauts would avoid negative short-term side effects associated with bisphosphonate administration that might be experienced while in space. This pre-treatment strategy would also mean that an actual inflight animal study of BP efficacy could be run with minimal astronaut work needed.

The two bisphosphonates chosen were alendronate and risedronate, as they differ in both binding affinity and anti-resorptive potency [13][14]. Both drugs are hypothesized to at least mitigate, and likely protect against, hindlimb unloading related bone loss. The effects of these drugs may also persist into the reambulation period. Their

performance in both periods will be assessed through CT scanning for densitometric and geometric properties and mechanical testing for the mechanical properties. This will hopefully give a better idea of which CT derived parameters show trends most similar to mechanical properties.

Another important aim of this study is to compare the performance of these two BPs in a pre-treatment scenario. Alendronate's effects are hypothesized to persist longer into the recovery period after withdrawal due to its greater binding affinity. If formation is suppressed due to the suppression of resorption BPs cause, then persistence of that antiresorptive effect into the recovery period could be detrimental. Risedronate's lower binding affinity may be advantageous in that case. Risedronate also has greater potency, which means it may provide better protection during the unloading period. There may be other differences in efficacy between the treatments based on type of bone (cortical or cancellous). The analyses conducted allow characterization of both of these types of bone tissue (separately and together). Knowing a treatment was more effective in preserving mechanical properties or the densitometric properties of a specific region could potentially allow more targeted treatment of osteoporosis and long-term bedrest patients.

1.1 Objectives

The purpose of this study was to examine the efficacy of BP pre-treatment in preserving bone densitometric, geometric, and mechanical parameters over an HU period and a recovery period. For this part of the larger study, the specific aims were to answer the questions:

(1) Do these BPs when administered as pre-treatments protect or mitigate the deleterious effects of HU at the DFM?

(2) Are the bisphosphonates more effective in specific bone region types (cancellous or cortical) or are they equally effective in both?

(3) Does a pre-treatment approach limit the persistence of their benefits or will they continue to benefit bone in the DFM into the 56 days of reambulation recovery?

(4) Do the estimated mechanical properties (from RPC testing) correspond well to the densitometric/architectural parameters (from μCT) for the cancellous compartment of the DFM?

(5) Do the two bisphosphonates, alendronate and risedronate, differ with respect to questions (1)-(4)?

Information available suggests that BPs will be effective even when administered as a pre-treatment, but their performance in specific regions is less clear. It is also hypothesized that risedronate will be more effective during the unloading period due to higher anti-resorptive potency. Alendronate is expected to persist longer into recovery. Persistence of BP effects could manifest as protection against the age-related losses the control groups, particularly ambulatory controls, could experience during the recovery period. However, these effects could also manifest in poorer parameters compared to controls because bone recovery is tied to formation which can be impaired with BPs administration.

2. BACKGROUND

2.1 Basics of Bone Function and Structure

The skeleton provides structure and supports the loading the body experiences from gravity and external sources. The magnitude and type(s) of loading a bone experiences is determined by both its location in the body and its use in movement. There are two main types of bone, cancellous and cortical, which have different mechanical properties based on structural and tissue level differences.

Bone tissue in both cancellous and cortical bone is composed of inorganic crystalline minerals, collagen fibers, and water [8]. Aligned collagen fibers and mineral crystals form fibrils that combine with extrafibrillar minerals into fibers that form lamellae. Fiber orientation varies between lamellae and can regionally orient to increase tensile strength. Mineral content is greater in cortical bone than in cancellous bone but it tends to vary little through a cross-section of cortical bone. The differences in mineral content and ability of the fibers to align consistently are tissue level differences between the two types of bone.

Cortical bone has low porosity and contributes the strength and stiffness to bone. The functional unit of cortical bone in humans is the Haversian system which consists of several layers of concentric cylindrical lamellae surrounding a channel. These channels which are called Haversian canals surround blood vessels and nerve cells. Haversian systems, also called osteons, are oriented along the bones' longitudinal axis and have interstitial lamellae between them. Figure 2 shows bone structure including a raised osteon and labels for different features.

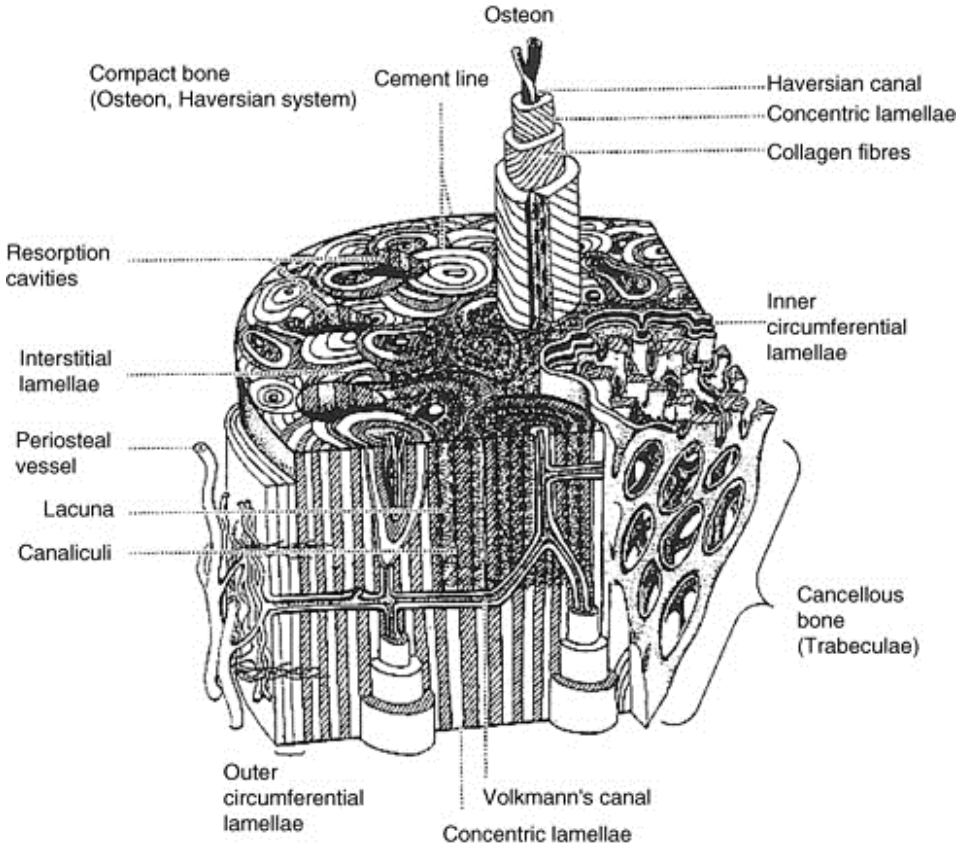

Figure 2: Diagram of the Two Types of Bone and Their Important Features. Reprinted from Jee's *Cell and Tissue Biology: A Textbook of Histology* [15]

Rat cortical bone differs from human cortical bone in that it lacks Haversian systems. This somewhat limits the applications of a rodent model to investigating cortical mechanical properties. In non-human bones that have Haversian systems, greater proportions of Haversian bone correlate to lower strength (tensile, compressive, shear, and bending) and stiffness [8].

Cancellous bone has a highly porous microarchitecture that behaves mechanically like a solid open celled foam. The individual struts that make up the scaffold of cancellous bone are called trabeculae. It contributes less strength than cortical bone, but is valuable for the energy absorption abilities that come from its structure. Two factors that contribute to the inferior strength of cancellous bone are the lower mineral content and density of the bone tissue.

Bone has a composite structure that can differ by location to accommodate greater strain experienced at specific sites. The ratio of cancellous to cortical bone is the main difference with vertebra and the ends of long bones having a greater cancellous portion [12]. Conversely, midshafts of long bones like the femur and tibia are almost entirely composed of cortical bone. Mixed bone sites would have both strength from the cortical contribution and energy absorption abilities from cancellous.

2.2 Remodeling and Loading Response

The two processes by which bone is changed are called modeling and remodeling. In each process, there is both bone resorption and formation though the balance and coordination of those two differ [8]. During modeling, formation and resorption need not be coordinated and may be imbalanced. The balance can be shifted towards greater formation or greater resorption as necessary to accommodate loading. Formation and resorption can also occur at differing sites so that bone is in effect reshaped. Modeling allows for both growth and reshaping needed for development prior to skeletal maturation. Modeling rate tends to tail off quite a bit after skeletal maturity is reached since it is greatly related to skeletal growth and maturation.

Remodeling occurs as part of normal bone metabolism which is involved in skeletal maintenance and some load adaptation. During remodeling, formation and resorption occur at nearby sites on the surface. There is also greater balance of those two activities. Maintenance is one aspect of remodeling and is needed to repair the fatigue damage that bone naturally accumulates over time. Adaptation related remodeling occurs when the bone's strain is increased or decreased due of changes in body weight or exercise level. Both cortical bone and cancellous bone undergo remodeling but the rate of remodeling can differ between the two regions.

The steps of remodeling are activation, resorption, and formation which are shown in Figure 3. The cells involved in the process are osteoclasts which resorb bone and osteoblasts which lay down new bone [8]. Osteoclasts in the basic multicellular unit (BMU) form in response to a mechanical or chemical signal during the activation phase. They attach to the bone and resorb in the area immediately around them until the

intended volume has been removed. Osteoblasts form near the end of resorption and initiate the formation stage which proceeds far slower than resorption. In the case of modeling, Figure 3 might depict greater degrees of formation compared to resorption or vice versa. It could also show formation occurring at the surface opposite to resorption as is the case in reshaping.

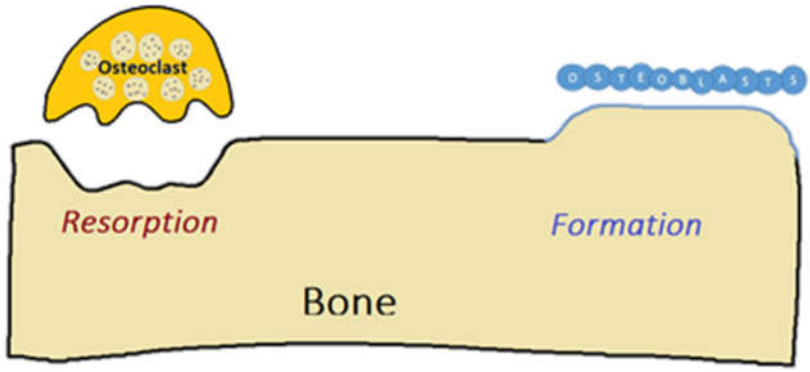

Figure 3: Osteocytes and Their Presence and Use in the Remodeling Process

During space travel, astronauts experience drastically reduced gravity which bone interprets as a situation of reduced strain. The body responds by remodeling bone to fit the lowered demands of microgravity which primarily means there is increased resorption. Astronauts tend to experience decreases in bone mineral content, bone mineral density, and cross-sectional geometric parameters [1]. Returning to earth's gravity triggers increased formation, however, formation takes longer than resorption does. In the meantime, astronauts may be at an increased fracture risk due to their unsuitable bone properties [16].

The strain based model of bone adaptation, called the Mechanostat model, was developed by Harold Frost. It is a proposed alternative to Wolff's law that attempts to explain the mechanosensitivity of bone [17]. In this model, there is an equilibrium range of strains that do not trigger either increased remodeling or modeling [8]. Increased resorption occurs when bone experiences extended periods of reduced strain due to disuse or decreased loading [18]. Conversely, periods of increased strain will signal for

increased modeling. One consequence of this in cancellous bone would be a sparseness or lack of trabeculae in areas of low strain due to loading type.

2.2.1 Bisphosphonates' Effect on Remodeling

Bisphosphonate treatments are typically used to combat conditions where there is an imbalance in remodeling resulting in excess resorption [19]. During osteoporosis, resorption occurs despite strain levels being more appropriate for bone maintenance. Bisphosphonates are deposited into bone tissue where they bind to mineral crystals and are later resorbed by osteoclasts. The non-nitrogen containing versions of these drugs cause osteoclasts that resorb them to undergo apoptosis [13]. Nitrogen containing bisphosphonates instead interfere with farnesyl diphosphate synthase (FPPS) [13]. Affected osteoclasts remain on the bone surface, but no longer actively resorb bone. In effect, these osteoclasts are deactivated and resorption is decreased.

The decreased osteoclast count or activity reduces resorption and remodeling based formation due to the coupling of those two during remodeling. In osteoporosis patients, this leads to improvements in bone density and mechanical performance as quantified by decreased fracture risk. Bisphosphonates can also be used to reduce resorption in cases where increased resorption would be appropriate based on the mechanostat model. For astronauts, drug treatment would reduce the increased osteoclast activity triggered by microgravity exposure and either mitigate or prevent expected losses.

Two key aspects influencing a particular bisphosphonate's efficacy are antiresorptive potency and binding affinity. Antiresorptive potency refers to their ability to inhibit osteoclast activity either by causing osteoclast apoptosis or by deactivating them. Greater antiresorptive potency means better osteoclast inhibition. Binding affinity refers to their ability to bind to HAP and thus the amount of the drug retained. Greater binding affinity means more of the drug is deposited into bone and it tends to have greater retention time. Lower binding affinity drugs appear to penetrate further into the bone which may mean they preferentially bind to greater surface area locations like

cancellous bone [13]. Overall performance is likely a balance of binding affinity and antiresorptive potency.

Bisphosphonates that successfully bind to the bone work until one of two things occur. They stop working once they have been buried by newly formed bone and only affect the osteoclast they are resorbed by [19]. Administering the bisphosphonates regularly in a state of normal bone maintenance would allow deposition in the outer layer and newly formed layers. This could allow astronauts to be pre-treated prior to space travel because some layers of bisphosphonate containing tissue would persist into resorptive state. The length the effect would persist would depend on osteoclast activity and how much of the drug deposited into the layers of bone.

2.3 Mechanical Properties of Cancellous Bone

Mechanical testing of cancellous bone to estimate intrinsic properties poses a unique problem. Cancellous bone is heterogeneous, anisotropic, and structurally an open celled solid foam [20]. All bone, cancellous or cortical is also viscoelastic and thus are strain rate dependent. Open celled foams have unique looking stress strain curves due to having three regions of different behavior as shown in Figure 4.

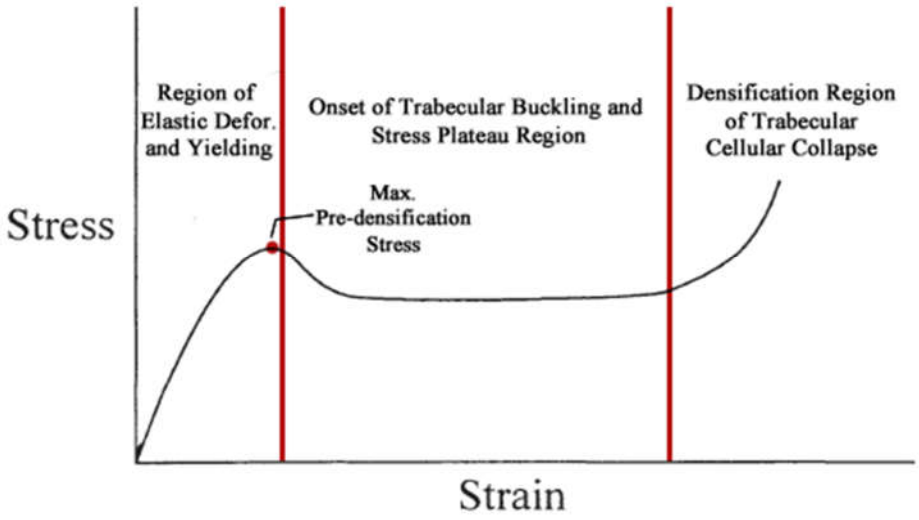

Figure 4: Stress-Strain Diagram Showing Major Regions Separated by Lines and the Location of Maximum Pre-Densification Stress. Reprinted from Martin, Sharkey, and Burr's *Skeletal Tissue Mechanics* with additions [8]

In the initial region, individual trabeculae elastically deform until they reach their yield point [16]. After yielding, there is a region where stress has plateaued during which the trabeculae begin to buckle [21]. Cells begin to collapse once buckling has onset which causes the material to densify and force to increase rapidly. In this densification region, the material has already failed and is just compressing the remaining space out of the failed structure.

There are two types of properties yielded by analysis of the mechanical testing data. Intrinsic properties like elastic modulus (E) or ultimate stress (σ_{ult}) are theoretically independent of geometry. Extrinsic properties like stiffness (k) or max pre-densification force (F_{ult}) depend on the specific geometry of the material tested. There are some limitations to determining these properties for a very porous material like cancellous bone. Three major concerns are end effects, heterogeneity, and treatment as a continuum material.

End effects result from machining cross sections of bone and disrupt the trabecular network that would have supported trabeculae on the exposed surface [8]. During a compression test, the platens would be pressing against these possibly damaged trabeculae which would show in the test as poorer performance. This can occur both at the sides if the specimens are cored as well as at the top and bottom. Cancellous bone is also very heterogeneous which means that within even small samples there can be variations in structure that influence strength. The yielded properties would depend on the weakest area which makes those values a poor representation of the average properties.

A final concern is that getting a sample cancellous bone large enough to be considered a material continuum for analysis is not possible for a small species like rats [22]. The scale needed to qualify as a continuum is larger than is feasible especially in the long bones. Samples must be instead thought of as a structure rather than a continuum and their mechanical properties as an estimate for the structure which may differ from a continuum. These concerns do not make the data gathered through reduced

platen compression tests (detailed in future sections) less valuable. It does mean that the intrinsic properties are an estimate and one that is affected by these limitations.

2.4 The Hindlimb Unloading Rat Model

Ground based models to simulate microgravity exposure an important tool that allows researchers to study the effects on the body without needing to go to space. More studies can be done and there is more freedom in what is possible for the study design. Ground studies are less limited in how long they can last, and can be more animal work intensive. By far the most popular rat model is the hindlimb unloading model described by Morey-Holton [1].

The model involves harnessing the rat's tail and lifting their hindlimbs by hoisting their tail. Once lifted, the torso of the rat should be at a 30º angle with the cage floor. This model does induce cephalad fluid shift and changes to some bones and muscles similar to what astronauts experience [23]. One large difference is that the forelimbs of the rat are not unloaded; thus, musculoskeletal changes in them would be limited compared to weight bearing limbs. Previous studies by Shirazi et al. suggest that 28 days of unloading adult rats with this model yields losses similar to those seen in astronauts after 4-6 months [24]. Twenty eight days of unloading thus is a useful time range for examining bone and other physiological changes that astronauts on the ISS would experience.

Some limitations to the model make certain bone sites like the upper spine and the mandible experience changes dissimilar to those experienced by astronauts. One major consideration for the rat model is that rat cortical bone differs from human cortical bone. As noted in a previous section, rats lack Haversian systems which some believe rats do not undergo aging related osteonal remodeling. Adult rat cortical bone would thus not see the decreased strength due to normal skeletal maturation. This premise has proven false as older rats (i.e. 8 months or older) have shown signs of intracortical remodeling [25].

Skeletal maturity in rats is reached at around 6-7 months [26]. This would mean age related decreases in strength under consistent conditions would likely not occur until

a month after maturity. Humans would instead see losses in strength with increased Haversian bone throughout their growth. The consequence is that observed cortical changes especially in mechanical properties may not be incredibly similar between the species. Changes in BMC, BMD, and geometric parameters for the cortical region could also correspond poorly to astronauts. This specific limitation would not extend to the cancellous region which is more similar in structure and composition between species though scaling differs.

3. METHODS

3.1 Experimental Design

The effects of simulated microgravity and treatment efficacy were evaluated using the adult hindlimb unloaded (HU) rat model. Five and a half month old Sprague Dawley rats were purchased from Harlan Sprague Dawley Inc. (Houston, TX) so that they would be skeletally mature after a two-week acclimation. These animals were part of a Texas A&M University Institutional Animal Care and Use Committee (IACUC) approved animal protocol for a study. As mentioned previously, the rats studied in this thesis were a part of a larger project with four (two anti-catabolic and two anabolic) pre-treatments. However, the scope of this thesis is limited to the two bisphosphonate (BP) anti-catabolic pre-treatments. The purpose of the broader project is to examine the efficacy of each of the four options when a pre-treatment approach is taken. Their efficacy over both the HU period and a subsequent recovery period was assessed using peripheral quantitative computed tomography (pQCT), micro-computed tomography (μCT), and reduced platen compression (RPC) mechanical testing.

The overall study design was devised to include the other parts of the project as well as a broad suite of outcome variables. A schematic of the basic study design with a timeline and endpoints is depicted in Figure 5. The age of the animals is also denoted above the timeline. The nominal start of the experiment timeline is day 0, denoted as baseline, which follows the 2-week acclimation period. Phases of the study in chronological order are as follows: pre-treatment for 28 days, unloading for 28 days, and recovery for 56 days of return to normal ambulation. Although not included in this thesis work, it should be noted that *in vivo* pQCT scans of the proximal tibia metaphysis (PTM) were taken every 28 days starting at baseline. These scans taken at baseline were used to block assign the animals into four groups of roughly equal average body weight and total volumetric bone mineral density at the PTM (from the scans) with two control and two treatment groups. Ambulatory controls (AC) received no pre-treatment nor underwent unloading. Hindlimb unloading controls (HUC) also received no pre-

treatment but did undergo a period of hindlimb unloading. The two pre-treatment groups studied in this thesis work were administered the bisphosphonates alendronate (ALN) and risedronate (RIS). Both RIS and ALN groups were treated and unloaded. All 3 HU groups returned to normal cage ambulation for 56 days following HU.

Table 1 summarizes the four groups and details the number of rats terminated in each group per time point. This half of the study did have an unbalanced design which is particularly noticeable in the control groups. More control animals and their data will be added to these groups during the second half of the larger study. Groups denoted with hyphens were not different in condition from ambulatory controls at that point. For example, at baseline, no groups have been treated or unloaded so HUC, ALN, and RIS groups were not different from AC. To assess bisphosphonate efficacy, left femurs were excised for *ex vivo* analysis at the time points indicated. They then underwent peripheral pQCT scanning, μCT scanning, and RPC mechanical testing of the distal metaphysis. The time points of interest were at baseline (day 0), at the end of pre-treatment (day 28), at the end of unloading (day 56), and at the end of recovery (day 112).

Figure 5: Study Timeline and Major Time Points

Table 1: Animals Terminated Per Group at Each Time Point

	Day 0	Day 28	Day 56	Day 112
AC	7	8	6	8
HUC	-	-	9	10
ALN	-	15	14	14
RIS	-	16	12	17

3.1.1 Details of Animal Work

During the rats' two-week acclimation, they were held and handled regularly to get them accustomed to regular interaction. This made handling them for scanning, injecting, and harnessing easier and likely less stressful for the rats. Day 0 scans of the tibia metaphysis follow, and the total vBMD from these was used in combination with body weight to block assign rats into the four groups. A figure showing these body weights appears at the beginning of the results section below. Rats were single housed for the length of the study and were housed in shoebox cages throughout the experiment except during the HU period. They were fed standard rodent food (Harlan Teklad 8604) ad libitum and were not limited in their water intake.

During the 28-day pre-treatment period, the RIS and ALN groups were given subcutaneous injections three times a week. The doses of RIS and ALN administered were 1.2 μg/kg and 2.4 μg/kg, respectively, which were meant to mimic the clinically relevant dose for treating osteoporosis. Specifically, these doses were designed to correlate with the 35 mg/week and 70 mg/week doses used to treat women with postmenopausal bone loss [27][28]. All groups including HU and ambulatory controls were weighed twice a week during the pre-treatment period. They were scanned again at the end of this period and all groups besides AC were harnessed for hindlimb unloading.

The RIS, ALN, and HUC rats were hindlimb unloaded according to a modified version of the Morey-Holton procedure [1]. The tail harness differs and an illustration of the modified version can be seen in Figure 6(a). The paperclip hook at the end of the harness is attached to an overhead pulley and rod system in Figure 6(b) to achieve a 30º head-down tilt. Rats could ambulate normally on their forelimbs to access food and water during the HU period.

Health checks were performed twice daily to look for signs of self-inflicted bite wounds to their tail or damage to their harnesses. If damage was found, they were fitted with a cone on the tail to protect the area and any wounds were treated with an antibiotic plus analgesic cream. HU cages were cleaned and rats were weighed twice weekly. Weight monitoring was important because a 10% decrease in body mass was grounds for

removing an animal from the study. No rats were removed from the study due to weight loss. However, there were two animals removed due to concerns over their tail conditions. Two more were removed due to chewing off their harnesses and spending more than 8 hours fully weightbearing before they could be reharnessed. These animals were not counted for the animals numbers reported in Table 1.

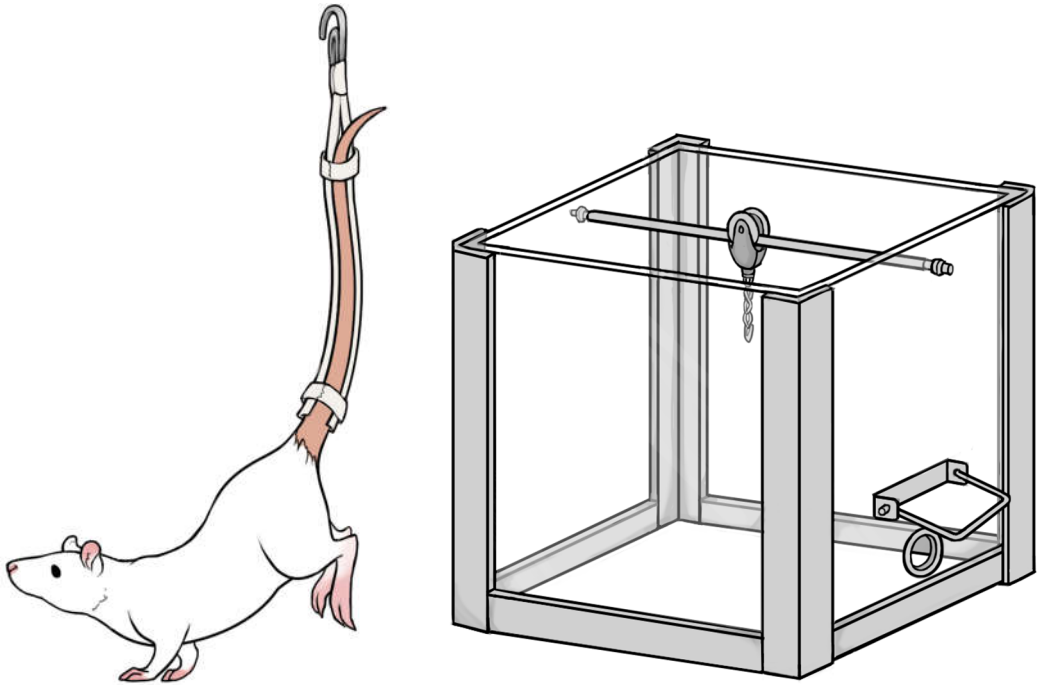

(a) **(b)**

Figure 6: (a) Diagram of a Harnessed and Unloaded Rat & (b) Custom HU Cage

After the end of the unloading period, rats were scanned by pQCT and their harnesses were removed. The groups who underwent hindlimb unloading then returned to normal ambulation in standard cages for recovery. The recovery period lasted 56 days during which rats were weighed twice a week. The three HU groups were monitored more extensively during the first week to assure that they were healthy after the transition. At the end of the recovery, the remaining animals were scanned and then there was the final round of terminations on day 112.

3.1.2 Bisphosphonate Choice and Characteristics

Bisphosphonates can differ in many ways, but two key aspects in which they can differ are their binding affinity and antiresorptive potency. Both of these properties are important to consider when using BPs to prevent microgravity related bone loss. The two BPs used in this study, alendronate and risedronate, have differing binding affinities and antiresorptive potencies. The difference in potencies is addressed at least partially by the difference in dose administered. Alendronate has the greater binding affinity of the two, while risedronate has the greater antiresorptive potency.

Risedronate with its higher potency was chosen for its strength in inhibiting osteoclast activity and thus reducing resorption. However, due to its lower binding affinity, risedronate uptake by bone is poorer and its effects may persist for a shorter time. Alendronate was selected for its binding affinity that makes its use as a pre-treatment approach very feasible. Greater amounts of alendronate should bind to and be retained by bone. Alendronate's effects would likely persist longer as a result. For a pre-treatment approach to protecting bone, two characteristics would make a specific BP a more suitable choice. They could be chosen for their overall protective strength (risedronate) or the length of their effect's persistence (alendronate). The BP choices in this study suit these two different selection criteria.

3.2 Computed Tomography

3.2.1 Peripheral Quantitative Computed Tomography (pQCT)

Ex vivo peripheral quantitative computed tomography (pQCT) scanning of the distal femur was used to assess bone densitometric and geometric properties. A Stratec XCT 3000 (XCT Research M Stratec; Norland Corp., Fort Atkinson, WI) was used to scan harvested femurs with a voxel size of 0.07 mm. Bones were placed in a plastic holding tube filled with phosphate-buffered saline (PBS) for the scanning period. Scans were taken at both the femur diaphysis (FD) and the distal femur metaphysis (DFM). However, the metaphysis is the region focused on in this thesis work. At the metaphysis, four 0.5 mm thick slices are scanned starting 4.5 mm from a reference line located

midway between the condyles and the intercondylar fossa as shown in Figure 7(a). The reference line is labeled with R, and the cluster of four scans is labeled M1. One slice 0.5 mm thick was taken at the diaphysis of the bone which is positioned at half the total length of the bone relative to the reference line.

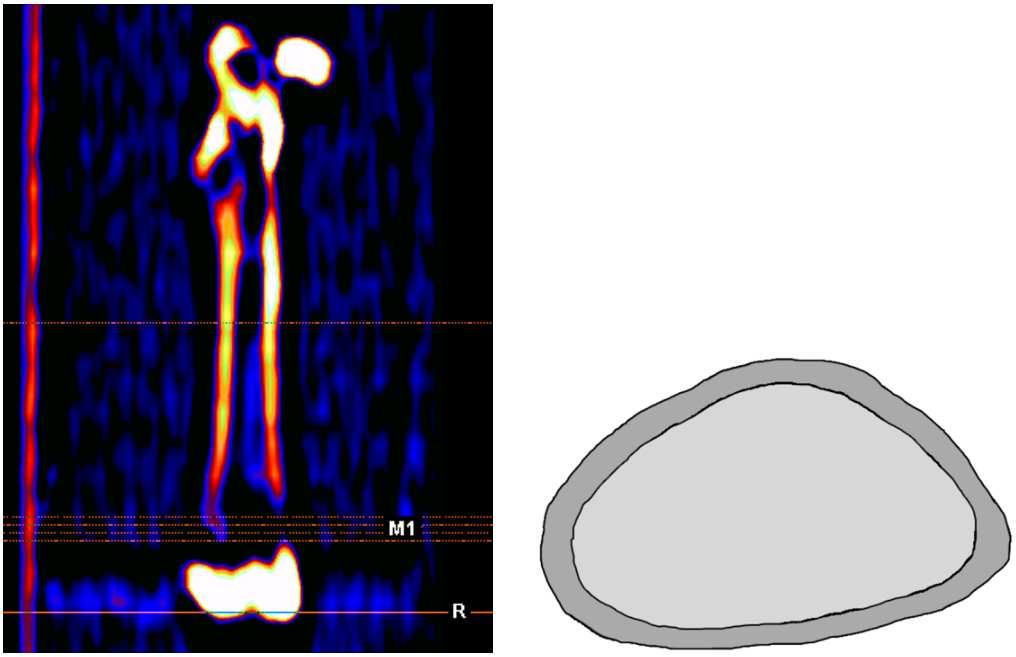

(a) **(b)**

Figure 7: (a) pQCT Scan Line Positioning; M1 Denotes Metaphysis Scan Lines and R Denotes the Reference Line. (b) Cross Section of DFM with Cortical Region in Dark Gray and Cancellous Region in Light Gray

The contouring and peeling algorithms used were native to the Stratec XCT software package (v6.00, Norland Corp., Fort Atkinson, WI). This contouring algorithm distinguished the outer edge of cortical bone from the surrounding PBS using thresholds of 450 and 650 mg/mm^3 for the DFM and FD, respectively. The endocortical surface, which divides the cancellous and cortical regions, is determined using peeling thresholds of 800 and 650 mg/mm^3 for the DFM and FD, respectively.

Custom excel VBA coded macros were used to isolate the parameters of interest from the total output and to average across slices at the same location. The bone densitometric parameters of interest were bone mineral content (BMC) and volumetric bone mineral density (vBMD) both of which were determined for the total bone, the cortical region, and the cancellous region as indicated in Figure 7(b). Note that the total bone region is the sum of cortical and cancellous regions and thus represents integral contributions from both types of bone tissue. BMC is the amount of mineral in the region of the slice per unit length of the bone (units of mg/mm). Normalization of BMC for the volume of the scan slice yields vBMD (units of mg/cm^3). Geometric parameters collected were the areas of those same three regions (total, cortical, and cancellous), the calculated cortical thickness (CCT), and the polar area moment of inertia (PAMOI). These outcomes will be used to assess changes in bone shape and composition as a whole at each time point.

3.2.2 Micro-Computed Tomography (μCT)

The distal femur metaphysis was also scanned using micro-computed Tomography (μCT) to analyze the cancellous region at a higher resolution. Higher resolution scans help show how changes in cancellous bone actually manifest in changes in the cancellous microarchitecture. Scanning and analysis into outcome data was performed by a collaborator, Dr. Larry Suva (Professor and Head, Department of Veterinary Physiology & Pharmacology, Texas A&M University). The scanner was a Scanco μCT 50 (Scanco Medical) with a voxel size of 6 μm. The scanned regions consist of 200 scans totaling a thickness of 1.2 mm, which is meant to correspond to the region compressed during RPC mechanical testing (details below). Specimens were thawed to room temperature and then placed into PBS filled specimen tubes for scanning.

The densitometric and architectural parameters collected were percent bone volume per total volume (%BV/TV), tissue mineral density (TMD), trabecular number (Tb. N), trabecular spacing (Tb. Sp), trabecular thickness (Tb. Th), connectivity density (Conn. density), and degree of anisotropy (DA). %BV/TV describes the proportion of

the total ROI volume of the cancellous region that is occupied by solid trabecular bone tissue and has units of percent (%). TMD is a measure of the true density of the mineralized bone tissue and it has units of mg/cm^3. Trabecular number (Tb. N) is specifically the average number of trabeculae per unit length (units of mm^{-1}). It is a derived parameter calculated using trabecular spacing. Trabecular spacing (Tb.Sp) is the average distance between trabeculae (units of mm). Trabecular thickness (Tb. Th) is the average thickness of the trabeculae within the ROI (units of mm). Both are assessed using 3D image techniques which fit spheres inside the appropriate structure on thresholded images.

Connectivity density (Conn. density) is a measure of the connectivity of trabeculae per tissue volume (units of mm^{-3}). It is derived from the Euler number which is itself calculated using 3D image techniques. Degree of anisotropy (DA) is the ratio of the maximum to minimum radii of the ellipse formed by the mean intercept length (MIL) plotted versus theta. Figure 8 shows this ellipse and its relation to the trabecular structure.

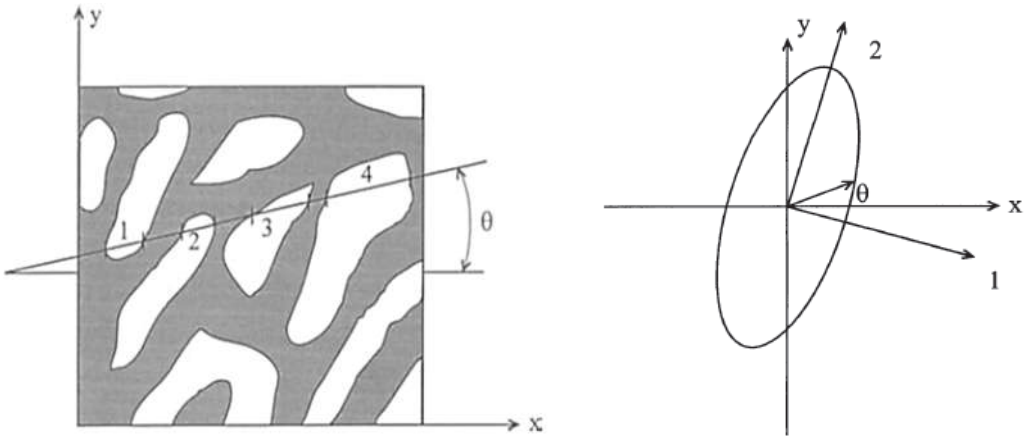

(a) **(b)**

Figure 8: (a) 2D Diagram of Trabecula Showing Theta Orientation (b) The Ellipse Formed by Plotting MIL vs. Theta (Max Radius Labeled as 2, Min Radius Labeled as 1) [8]

3.3 Reduced Platen Compression

Reduced platen compression (RPC) testing was used to estimate material (intrinsic) properties of the cancellous region of the distal femur metaphysis. Slices of the metaphyseal region are cut from the distal femur metaphysis, photographed, and sized for platens. The cancellous region is compressed by two circular platens to determine properties using the resulting force displacement data.

3.3.1 Specimen Preparation Method

Cross-sections 2 mm in height were cut from the distal metaphyseal region using a Well Precision Diamond Wire Saw model 3242 (Well Diamond Wire Saws, Inc., Norcross, GA) starting at the location shown in Figure 9(a). This location is based on the landmark of the most distal peak of the intercondylar fossa, which is the groove shown in Figure 9(b)

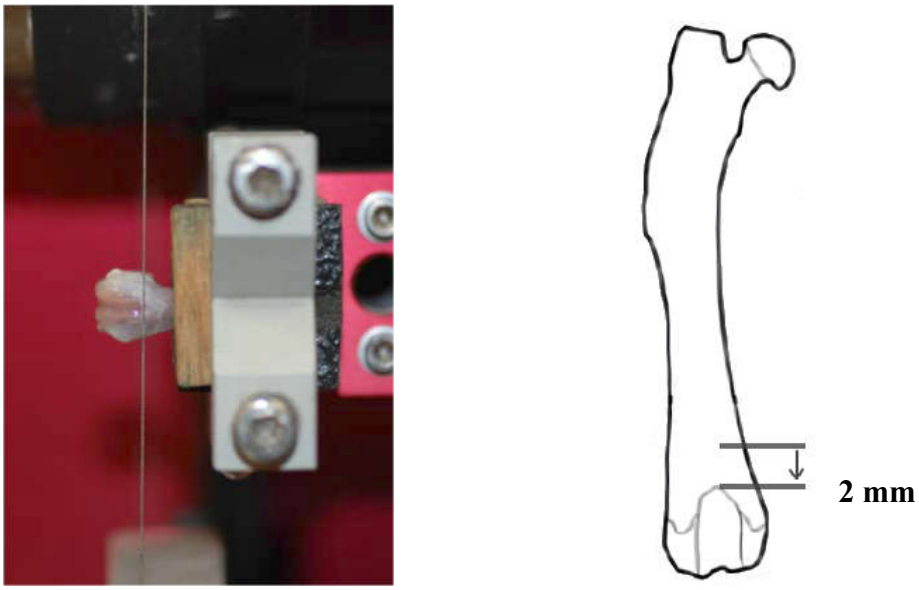

(a) **(b)**

Figure 9: (a)(b) Sawing Location of First Cut with Second Cut Closer Towards Midshaft

Sections were taken from a region similar to those scanned during μCT and pQCT. Once sectioned, specimens were photographed and then sized for platens using the image

processing software Adobe Photoshop (Adobe Systems Incorporated, San Jose, CA). Platen size was determined by taking 70% of the diameter of the largest circle inscribable within the endocortical region, which is termed the "endocortical circle" (Figure 10(a)).

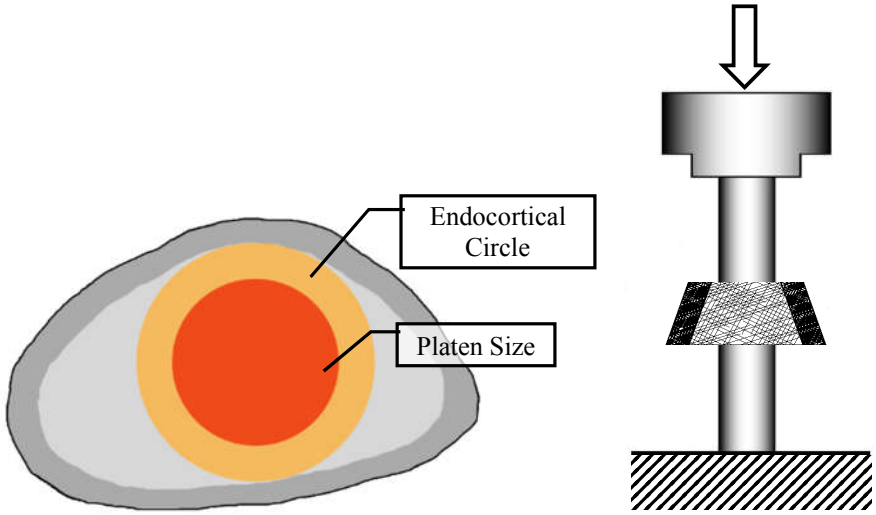

Figure 10: (a) Cross Section of DFM With Yellow Denoting Endcortical Circle and Orange Denoting 70% Circle & (b) Proper Specimen Placement and Platen Alignment

3.3.2 RPC Testing and Analysis Method

An Instron 3345 Single Column Testing System (Norwood, MA) with an attached 100N Instron load cell (2519-103, Norwood, MA) was used to compress the specimens using the appropriately sized platens. Both force and displacement data were collected at 20 Hz by the attached DAQ software Bluehill (version 2.35, Instron). The crosshead speed used for the compression test was 0.01 in/min (0.254 mm/min). Specimens were placed with the more distal side on the lower platen and the more proximal side being compressed by the top platen as shown in Figure 10(b).

Data were processed using a custom GUI based MATLAB (version 8.5, The MathWorks, Inc.) script which allows the user to indicate the elastic region and the densification point then outputs extrinsic properties. Variables of interest directly from

the load-displacement plots are maximum force (F_{ult}) and stiffness (k). The intrinsic properties of max stress (σ_{ult}) and elastic modulus (E) are estimated using platen area (A_{platen}) and Equations 1-2.

$$\sigma_{ult} = \frac{F_{ult}}{A_{platen}} \quad \textbf{(1)}$$

$$E = \frac{k}{A_{platen}} \quad \textbf{(2)}$$

The maximum force considered was the highest force prior to densification which is easily identified by a sharp increase in load after a period of little to no increase.

3.4 Statistical Methods

Statistical analysis of all assorted parameters was done using R (The R Foundation). The normality and homoscedasticity of the data for each parameter was evaluated prior to further analysis. The Shapiro-Wilk test was used to assess the normality and homoscedasticity was evaluated using a Brown-Forsythe Levene-type test. Once assumptions were evaluated, between-group comparisons appropriate for the data were conducted.

Between-group comparisons for parameters with normal homoscedastic data were made using a one-way ANOVA. If there was a significant difference, family-wise comparisons were made using Tukey-Kramer HSD post hoc test. Normal but heteroscedastic data were assessed first using a Welch's ANOVA and, if significant, then a Games-Howell post hoc test. Non-normal data were assessed using the Kruskal-Wallis rank sum test and multiple comparisons were evaluated with a Dunn's test.

4. RESULTS

All figures utilize line graphs with discontinuous lines joining the same groups at different time points. At each time point, the average values derive from a different set of animals since these data could be collected only after termination. Vertical error bars denote the standard deviation. The rectangular region with gray background denotes the hindlimb unloading period.

Body weight (BW) was monitored for each animal throughout the study to ensure health. Animals who lost too much weight (10% BW) especially over the HU period would be removed from the study. However, there were no removals for excessive weight loss. Figure 11 shows the group average weights each week with the HU period again denoted in gray. The greatest mean between-week loss in BW during the HU period occurred during the first week. This loss was greatest in the RIS group who lost 6.8% BW on average. Losses are a typical result of the rats getting accustomed to their changed living situation and the temporary increase in stress that accompanies.

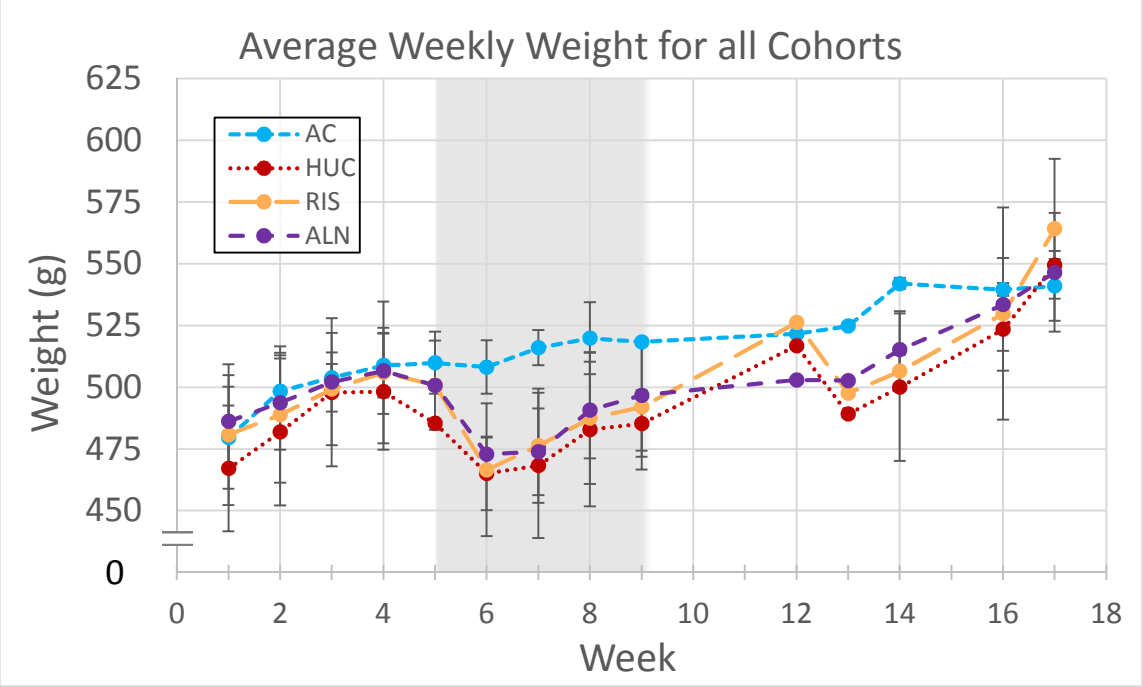

Figure 11: Group Average Weekly Weights Throughout the Study

The phrases "directly different" and "indirectly different" will be used throughout the results section. Directly different denotes two groups which are significantly different from each other. For example, if RIS were significantly different from ALN, then RIS would be directly different. Indirectly different denotes two groups who have different between-group differences in relation to the other two groups. For example, RIS and ALN would be indirectly different if RIS was significantly different from both HUC and AC, while ALN was only significantly different from HUC. In this example, RIS would be said to enhance a parameter while ALN would be said to protect it.

4.1 Computed Tomography (CT) of Distal Femur Metaphysis (DFM)

4.1.1 Ex Vivo *pQCT Results*

Table 1 summarized the number of animals per group terminated at each time point. However, technical error (mislabeled, missing, or leaking storage vials) meant some specimens were not available for *ex vivo* analyses. Accordingly, the number of bones actually used for *ex vivo* pQCT analyses has been summarized in Table 2.

Table 2: Specimens Available for pQCT per Group at Each Time Point

	Day 0	Day 28	Day 56	Day 112
AC	6	8	6	7
HUC	-	-	8	10
ALN	-	13	14	13
RIS	-	14	8	17

Bone Densitometry

All densitometric results for the distal femur metaphysis are organized by group and time point in Table 3 (pg. 31). All referenced figures appear after the body of the text in order of first mention. Following the unloading period total bone mineral content (BMC) (Figure 12) was significantly reduced in the HUC group (11.44 mg/mm) compared to AC (13.11 mg/mm). Both treatment groups were not different from AC.

Total bone mineral density (vBMD) (Figure 13) showed this same pattern of the treatments protecting against the losses HUC experienced compared to AC (523.4 versus 615.1 mg/cm^3). At the end of recovery, there were significant differences in vBMD but not in BMC. With a vBMD of 559.6 mg/cm^3, the HUC group was significantly lower than both treatments groups but not lower than AC.

Within the sub-regions of cancellous and cortical bone, the trends in densitometric parameters differed from each other and from the total region. In the cancellous region, BMC (Figure 14) for the HUC group was not significantly different from AC or RIS but was significantly lower than ALN following HU. ALN was significantly higher than HUC (5.19 vs 4.19 mg/mm) but was not different from AC. Cancellous vBMD (Figure 15) showed a more noticeable effect of HU with HUC being significantly lower than AC at day 56. Of greater note, the ALN group did not significantly differ from AC or RIS at day 56, but the RIS group had significantly higher BMD compared to AC (386.9 vs 340.0 mg/cm^3).

There were also significant differences between groups at d112 in the cancellous region. The AC group trended lowest in each parameter (i.e. cancellous BMC and vBMD). Though AC was lowest, HUC was not significantly different from AC in either cancellous vBMD or BMC. The ALN group had significantly higher BMC compared to AC (5.06 vs 3.63 mg/mm) but not to HUC (4.27 mg/mm) at day 112. For cancellous vBMD, the ALN group was not significantly different from either AC or HUC at day 112. In both parameters, RIS was significantly higher (5.48 mg/mm) than both HUC and AC but not significantly different from ALN. The results at both days 56 and 112 indicate that both drugs protect against the losses that the HUC group experiences in the cancellous region. However, RIS outperformed ALN, at least modestly, and outperformed the AC group.

The cortical region exhibits different trends than the cancellous region, however, cortical BMC showed a similar trend to total BMC. Like total BMC, cortical BMC (Figure 16) after HU was significantly lower for the HUC group as compared to AC (7.26 vs. 8.48 mg/mm) while the treatments were not. Following recovery, there was a

lack of significant differences between groups. In cortical vBMD (Figure 17), there were no significant differences at day 56, but there were some at the end of recovery. At day 112, AC had the highest vBMD which was significantly higher than RIS (1088 vs 1026 mg/cm^3). RIS, while lowest, was not significantly different from either HUC or ALN. It is likely that the higher cortical BMC of the AC group is related to lower turnover. The lower turnover experienced by the AC group would yield more mineralized bone especially in the cortex.

Table 3: pQCT Bone Densitometry Results

Baseline	Total BMC (mg/mm)	Total vBMD (mg/cm^3)	Cancellous BMC (mg/mm)	Cancellous vBMD (mg/cm^3)	Cortical BMC (mg/mm)	Cortical vBMD (mg/cm^3)
AC	13.7 (0.76)	643.2 (25.6)	5.27 (0.48)	398.7 (34.8)	8.42 (0.64)	1028.7 (26.7)
End of Pre-treatment (Day 28)						
AC	13.55 (0.94)	612.6 (30.5)	5.15 (0.60)	365.6 (40.9)	8.4 (0.58)	1028.7 (19.2)
ALN	13.62 (1.02)	632.8 (37.2)	4.91 (0.91)	368.0 (56.0)	8.71 (0.45)	1045.1 (29.2)
RIS	13.79 (1.25)	646.1 (37.3)	4.90 (1.06)	374.7 (64.3)	8.89 (0.62)	1050.2 (34.7)
End of Hindlimb Unloading (Day 56)						
AC	13.11 (0.84)	615.1 (26.9)	4.63 (1.05)	*340.0 (47.3)*	8.48 (0.30)	1056.5 (38.5)
HUC	11.44 (0.97) *	523.4 (36.0) *	4.19 (0.66)	*281.0 (19.6)* *	7.26 (0.87) *	1002.6 (50.9)
ALN	13.55 (1.17) †	607.4 (31.7) †	5.19 (0.85) †	*359.6 (32.2) †*	8.37 (0.79) †	1034.4 (35.8)
RIS	13.89 (0.77) †	639.5 (36.0) †	5.28 (0.68)	*386.9 (14.2) *†*	8.61 (0.85) †	1047.4 (34.4)
End of Recovery (Day 112)						
AC	12.83 (1.27)	*613.6 (79.1)*	3.63 (1.10)	279.9 (61.0)	9.21 (1.86)	1088.0 (47.0)
HUC	12.6 (1.47)	*559.6 (38.0)*	4.27 (1.01)	288.8 (39.1)	8.34 (0.82)	1040.0 (36.7)
ALN	13.57 (0.88)	*589.5 (34.0) †*	5.06 (1.04) *	334.3 (52.0)	8.52 (1.08)	1037.3 (45.8)
RIS	13.65 (1.32)	*603.9 (29.2) †*	5.48 (1.20) *†	365.3 (47.6) *†	8.17 (0.74)	1026.0 (43.2) *

Data presented as: Mean (Standard Deviation)
* - Significantly different from AC at $p < 0.05$
† - Significantly different from HUC at $p < 0.05$
# - Significant difference between treatments at $p < 0.05$
Italics indicates non-normal data assessed using Kruskal-Wallis with Dunn Post Hoc (Bonferroni Correction)
Red text indicates data which is non-normal and heteroscedastic

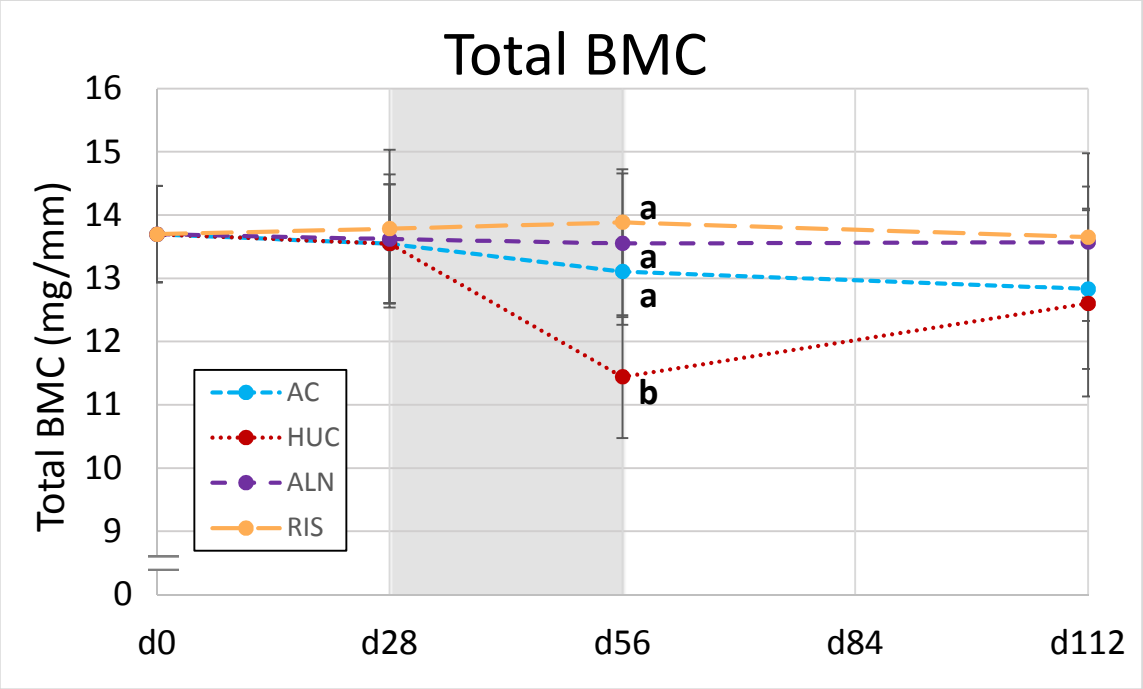

Figure 12: *Ex Vivo* pQCT Total BMC of Distal Femur Metaphysis

Hindlimb unloading period is denoted by gray rectangle. Groups not sharing a letter are significantly different from each other. Data are presented as mean ± standard deviation.

No significant differences existed at day 28 and all groups had similar average BMC. At day 56, HUC was significantly lower than AC, RIS, and ALN. No significant differences at day 112, but both treatment groups trended higher than control groups. Both treatments protected against the HU-related losses as evidenced by HU controls compared to AC.

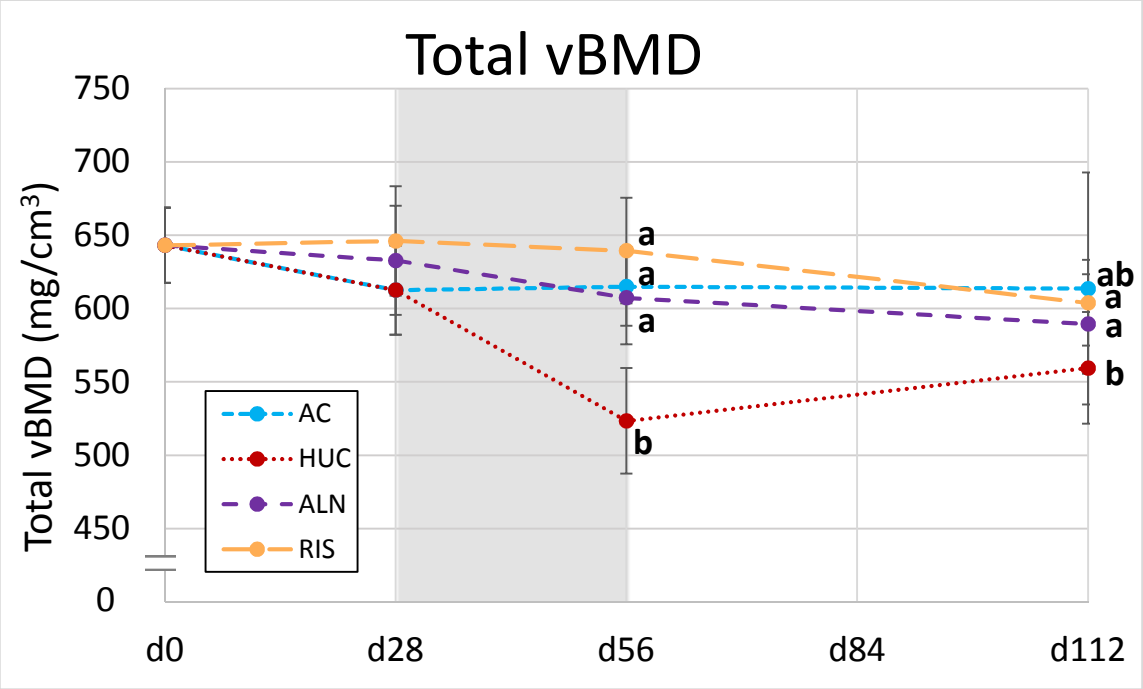

Figure 13: *Ex Vivo* pQCT Total vBMD of Distal Femur Metaphysis

Hindlimb unloading period is denoted by gray rectangle. Groups not sharing a letter are significantly different from each other. Data are presented as mean ± standard deviation.

After unloading, the HUC group was significantly lower than AC, RIS, and ALN. At day 112, HU controls were significantly lower than both treatments but not lower than AC. Both treatments protect total BMD through unloading. Persisting effects into recovery are difficult to assess as age related decline is not obvious here.

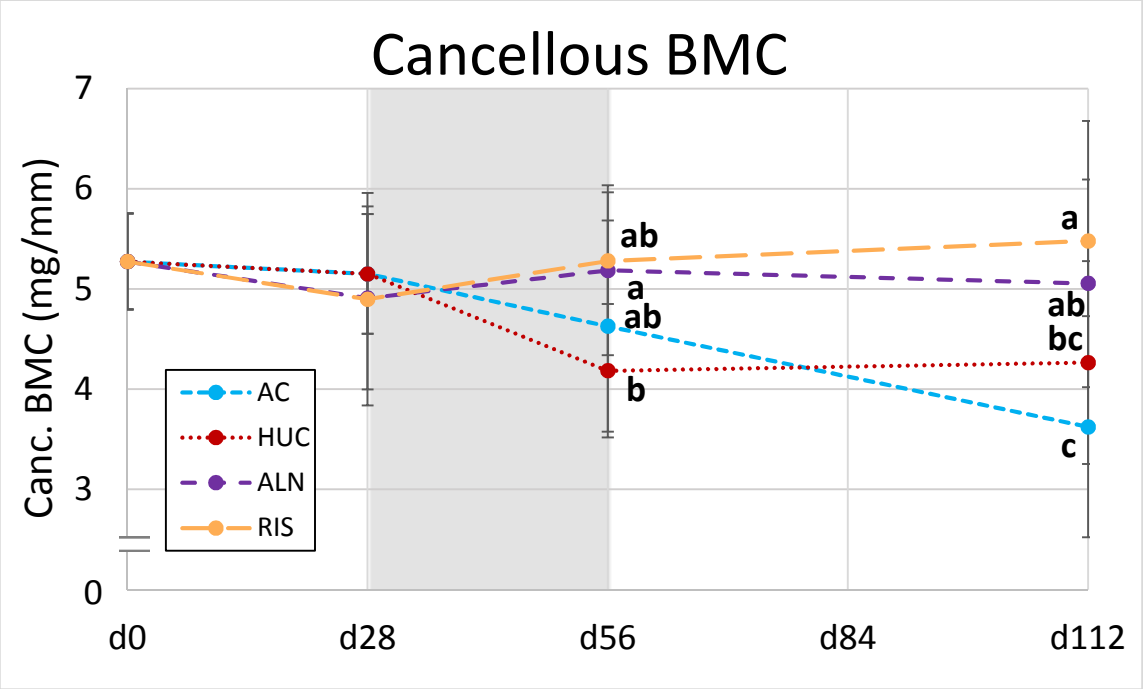

Figure 14: *Ex Vivo* pQCT Cancellous BMC of Distal Femur Metaphysis

Hindlimb unloading period is denoted by gray rectangle. Groups not sharing a letter are significantly different from each other. Data are presented as mean ± standard deviation.

At day 56, HU controls were significantly lower than ALN but not different from AC or RIS. At the end of recovery, AC is significantly lower than ALN and RIS but only trends lower (n.s.) than HUC. There seems to be an age-related decline that is attenuated somewhat by post HU recovery and protected against by both treatments.

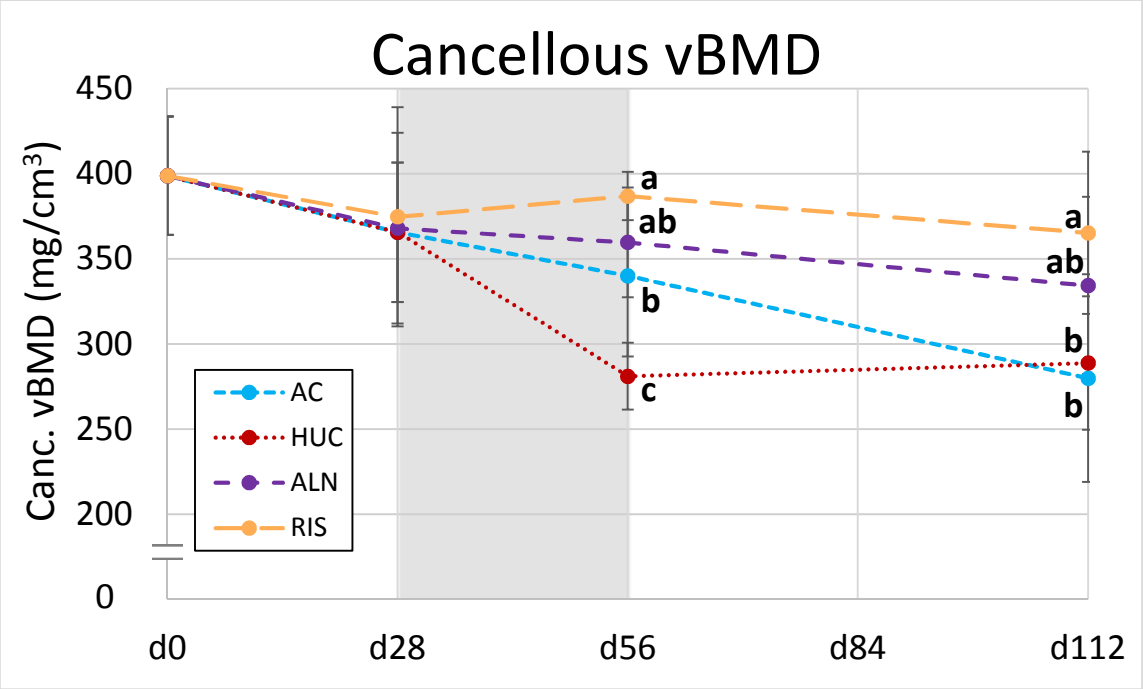

Figure 15: *Ex Vivo* pQCT Cancellous vBMD of Distal Femur Metaphysis

Hindlimb unloading period is denoted by gray rectangle. Groups not sharing a letter are significantly different from each other. Data are presented as mean ± standard deviation.

Normalization by marrow area changes the between-group differences at days 56 and 112 from those seen in cancellous BMC. HUC had lower cancellous vBMD at day 56 than AC, ALN, and RIS. ALN was not significantly different from AC but RIS was which indicates an indirect difference between treatments. RIS actually enhanced cancellous vBMD as compared to AC. At day 112, both controls groups do not differ from each other but are both lower than RIS. ALN was not different from RIS or either control groups.

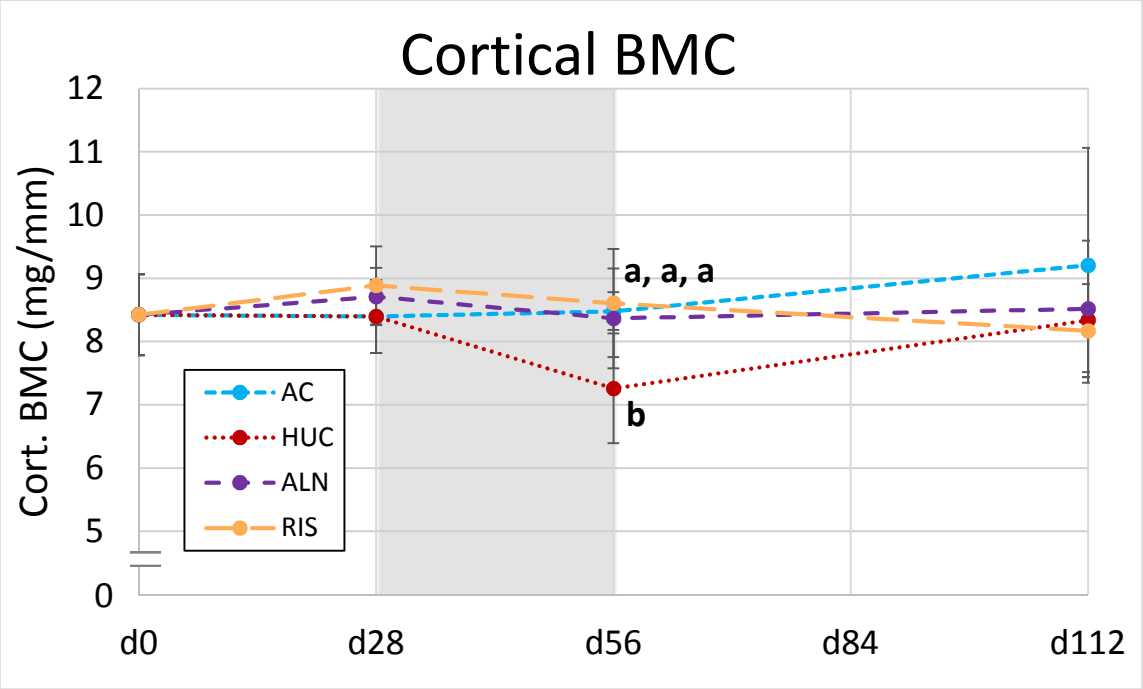

Figure 16: *Ex Vivo* pQCT Cortical BMC of Distal Femur Metaphysis

Hindlimb unloading period is denoted by gray rectangle. Groups not sharing a letter are significantly different from each other. Data are presented as mean ± standard deviation.

At day 56, HUC was significantly lower compared to AC and both treatment groups. No significant between-group differences existed at day 112 or day 28. Both RIS and ALN were effective at preventing losses in BMC that HUC experienced as compared to AC.

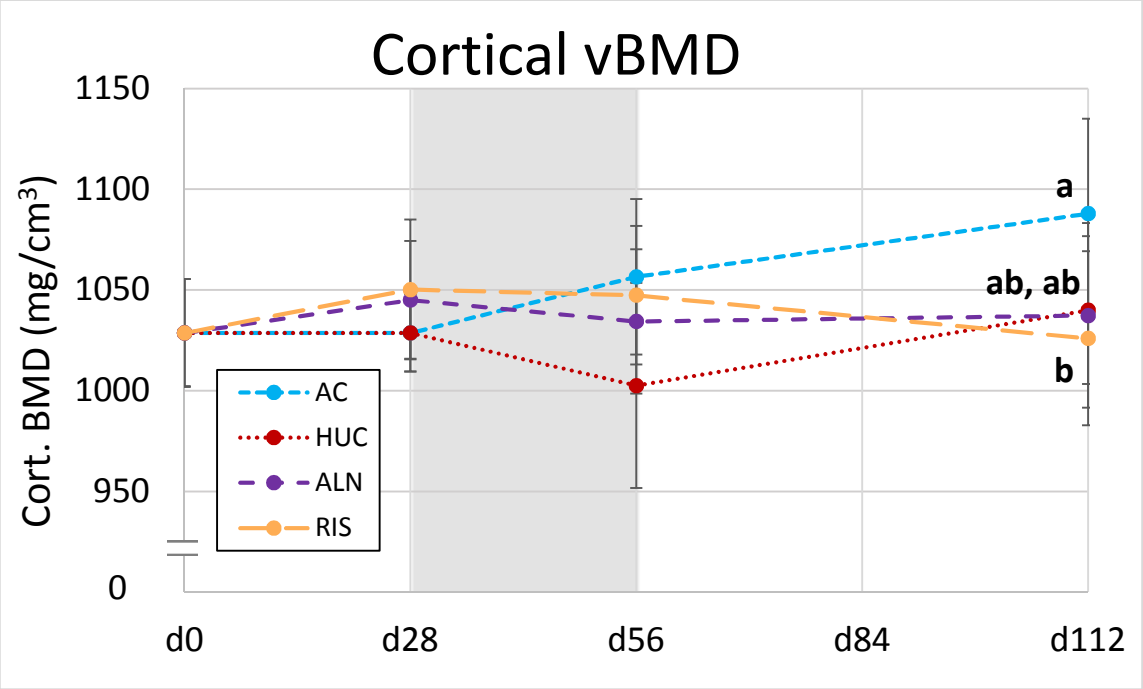

Figure 17: *Ex Vivo* pQCT Cortical vBMD of Distal Femur Metaphysis

Hindlimb unloading period is denoted by gray rectangle. Groups not sharing a letter are significantly different from each other. Data are presented as mean ± standard deviation.

At day 56, there were no between-group differences for cortical vBMD but there were differences at day 112. RIS had the lowest cortical vBMD, which was significantly lower than AC but not lower than ALN or HUC. Neither drugs could technically be said to protect during unloading since HUC did not significantly differ from AC at the end of HU (day 56).

Bone Geometry

All geometric parameter data collected at the distal femur metaphysis are organized by group and time point in Table 4. These geometric parameters are the ones used in normalization of BMC into vBMD and often account for differences in trends or lack thereof. The figures of all parameters with significant differences between groups for at least one time point appear below the text in order of mention.

Total area at days 56 and 112 did not significantly differ between groups. At day 56, the between-group differences in total BMC matched those of total vBMD. At the end of recovery, these differences did not match between BMC and vBMD despite the total area not differing. Endocortical area did not significantly differ at days 56 or 112 either; however, the non-significant differences did influence the cancellous vBMD (Figure 15). At day 56, these non-significant differences in endocortical area led to there being a statistically detectable difference in vBMD between the HUC and AC groups that is not seen in BMC. These differences also led to discernible difference in drug treatment performance that did not manifest in BMC. RIS had significantly greater cancellous vBMD than both control groups while ALN was only significantly higher than the HUC group. Both BPs protected from HU-related losses in the cancellous region. RIS had the highest BMC despite having the second lowest endocortical area.

Cortical area (Figure 18) for the HUC group was not significantly lower than AC following unloading; however, HUC was significantly lower than both treatment groups (7.22 versus ALN: 8.08 & RIS: 8.21 mm^2). At the end of recovery, there were no significant differences between groups. The between-group differences in BMC can be attributed to differences in cortical area at day 56 since vBMD does not differ. At day 112, normalization by the cortical area to obtain vBMD reveals differences not seen in BMC. Cortical thickness (Figure 19) showed similar trends to cortical area at both days 56 and 112 except for one difference. The difference was that the cortical thickness of the HUC group was significantly lower than AC following unloading (0.48 vs 0.55 mm). Unloading does appear to affect the cortical geometry more than it does the total or gross endocortical geometry.

Table 4: pQCT Bone Geometry Results

Baseline	Total Area (mm^2)	Endocortical Area (mm^2)	Cortical Area (mm^2)	Cortical Thickness (mm)	Polar Area MOI (mm^4)
AC	21.34 (1.56)	13.17 (1.23)	8.18 (0.50)	0.561 (0.026)	88.16 (12.31)
End of Pre-treatment (Day 28)					
AC	22.12 (0.81)	13.96 (0.54)	8.16 (0.53)	0.546 (0.031)	94.21 (6.66)
ALN	21.58 (1.68)	13.24 (1.40)	8.34 (0.46)	0.570 (0.026)	90.17 (13.28)
RIS	21.35 (1.52)	12.88 (1.29)	8.47 (0.59)	0.584 (0.039) *	88.76 (11.6)
End of Hindlimb Unloading (Day 56)					
AC	21.40 (1.98)	13.37 (1.85)	8.03 (0.22)	0.550 (0.026)	89.47 (15.13)
HUC	21.95 (1.67)	14.73 (1.58)	7.22 (0.60)	0.480 (0.043) *	91.75 (13.09)
ALN	22.35 (1.66)	14.27 (1.44)	8.08 (0.63) †	0.538 (0.041) †	95.77 (13.46)
RIS	21.77 (1.47)	13.56 (1.60)	8.21 (0.65) †	0.557 (0.054) †	90.14 (11.91)
End of Recovery (Day 112)					
AC	21.02 (1.12)	12.60 (2.17)	8.42 (1.30)	0.591 (0.128)	86.10 (8.58)
HUC	22.61 (2.78)	14.60 (2.31)	8.01 (0.71)	0.530 (0.035)	98.21 (23.40)
ALN	23.12 (1.46)	14.94 (1.51)	8.18 (0.70)	0.536 (0.055)	101.72 (11.99)
RIS	22.68 (2.24)	14.73 (1.96)	7.95 (0.58)	0.525 (0.04)	99.36 (18.38)

Data presented as: Mean (Standard Deviation)
* - Significantly different from AC at $p < 0.05$
† - Significantly different from HUC at $p < 0.05$
# - Significant difference between treatments at $p < 0.05$
Italics indicates non-normal data assessed using Kruskal-Wallis with Dunn Post Hoc (Bonferroni Correction)
Red text indicates data which is non-normal and heteroscedastic

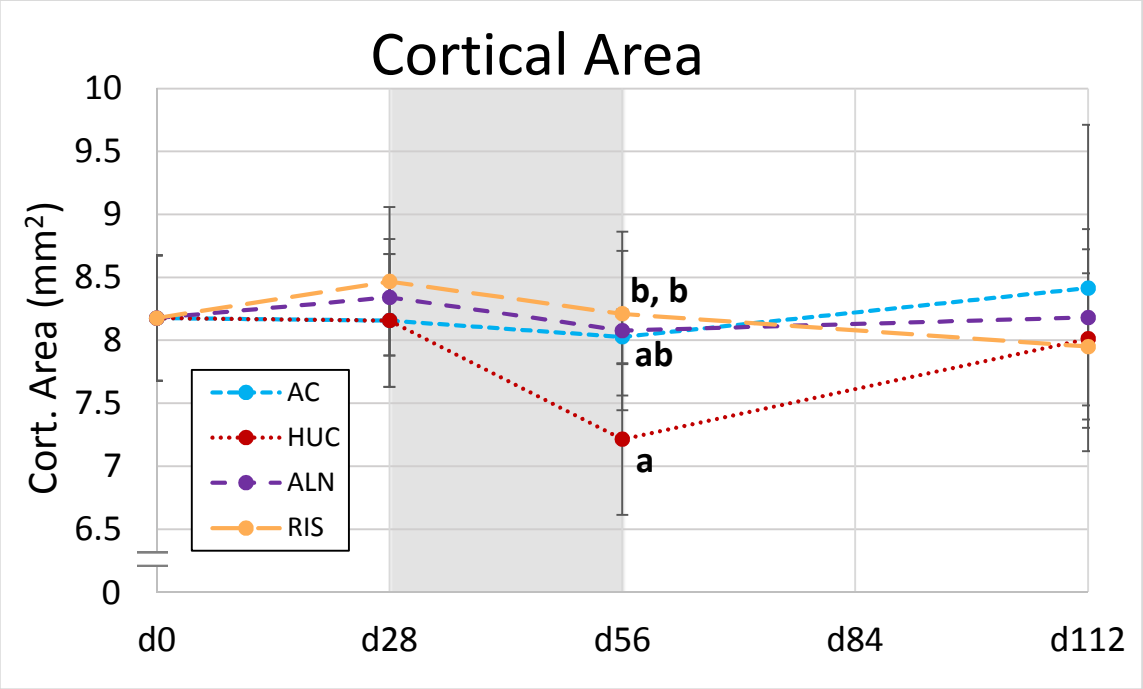

Figure 18: *Ex Vivo* pQCT Cortical Area of Distal Femur Metaphysis

Hindlimb unloading period is denoted by gray rectangle. Groups not sharing a letter are significantly different from each other. Data are presented as mean ± standard deviation.

After unloading, HU controls do not have significantly lower cortical area than AC. Both RIS and ALN were significantly greater than HUC which shows a positive drug effect. At day 112, there were no significant differences between groups.

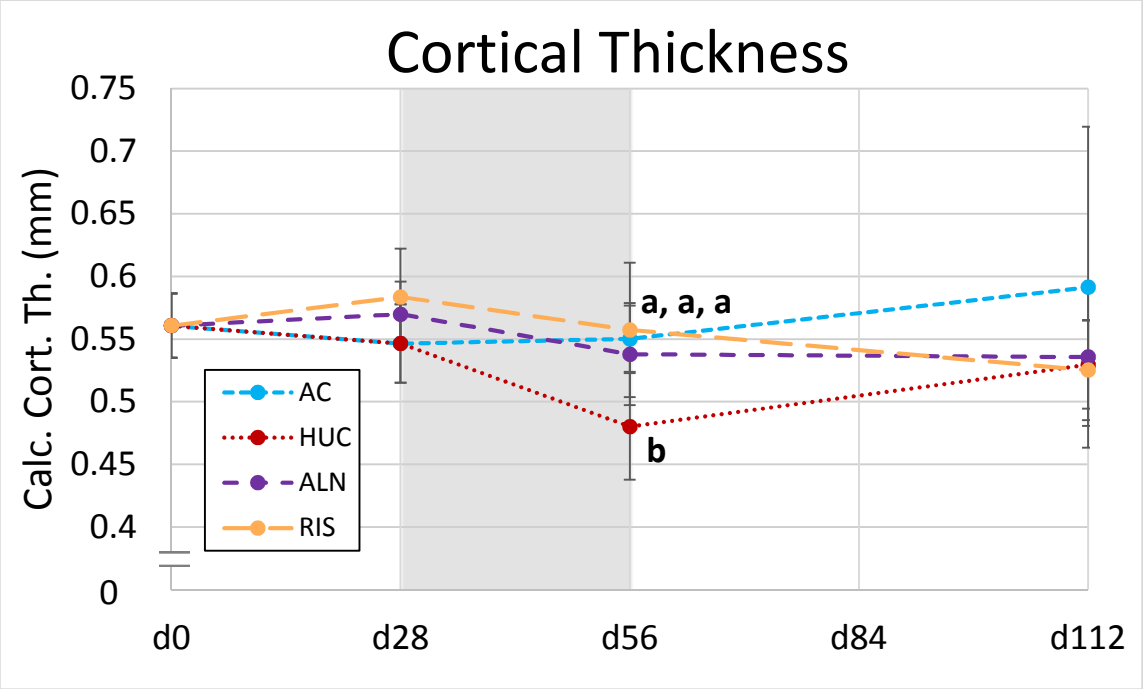

Figure 19: *Ex Vivo* pQCT Calculated Cortical Thickness of Distal Femur Metaphysis

Hindlimb unloading period is denoted by gray rectangle. Groups not sharing a letter are significantly different from each other. Data are presented as mean ± standard deviation.

At day 56, the calculated cortical thickness of HUC was significantly lower than AC and both drug groups. Again, both treatments protected against losses in calculated cortical thickness. After recovery, there were no between-group differences though AC trended higher than the other groups which followed the trend of cortical BMC.

4.1.2 Ex Vivo *μCT Results*

Micro CT scanning of the distal femur metaphysis allowed for higher resolution characterization of the trabecular compartment. The results are a mix of bone densitometry and trabecular architecture type outcome variables. The figures of all parameters with significant differences between groups appear below the text in order of mention.

Table 1 summarized the number of animals per group terminated at each time point. However, technical error (mislabeled, missing, or leaking storage vials) meant some specimens were not available for *ex vivo* analyses. Accordingly, the number of bones actually used for μCT analyses has been summarized in Table 5.

Table 5: Specimens Available for μQCT per Group at Each Time Point

	Day 28	**Day 56**	**Day 112**
AC	8	6	8
HUC	-	9	10
ALN	13	14	14
RIS	14	12	17

Densitometry

All μCT densitometric data collected at the distal femur metaphysis are organized by group and time point in Table 6.

Average %BV/TV (Figure 20) following the hindlimb unloading period (day 56) differed between the two control groups and between the two drug groups. RIS has significantly greater %BV/TV than all other groups. ALN and AC do not differ significantly from each other, but HUC was significantly lower than both were. At the end of recovery (day 112), there were no significant differences between RIS, ALN, and AC, but HUC was significantly lower than RIS. Both drug groups protected against the losses in %BV/TV experienced by the HUC group. Risedronate went beyond protection over unloading and appeared to enhance %BV/TV above controls.

TMD (Figure 21) is a measure of the mineralization level of the trabecular bone tissue that constitutes the solid part in the cancellous compartment. Thus, it is similar to cortical bone density. Directly after unloading, there were no significant differences between group mean TMD values. At the end of recovery, RIS was significantly lower than HUC (987.1 vs 1009.2 mg/cm^3) but not different from AC or ALN. The major difference from cortical vBMD is in the RIS group at day 112 which is different from HUC rather than AC.

Cancellous Micoarchitecture

All μCT cancellous microarchitectural data collected at the distal femur metaphysis are organized by group and time point in Table 7.

Trabecular number (Figure 22) directly after the unloading period was greatest for RIS (3.58 mm^{-1}), which was the only group that was significantly greater than HUC (2.95 mm^{-1}). Tb.N of ALN and AC did not differ significantly from either RIS or HUC, which was a trend also seen in trabecular spacing. In the case of Tb.Sp (Figure 23), the RIS group (0.27 mm) had the lowest average spacing and HUC (0.33 mm) had the greatest. HUC also had significantly lower trabecular thickness (0.08 mm) (Figure 24) at day 56 than all the other groups. Connectivity density (Figure 25) at the end of the unloading period showed the same trend as %BV/TV at day 56.

These results indicate both treatments were effective at maintaining trabecular structure comparable to ambulatory controls following unloading. These results also indicate that RIS performed slightly better since it was different from HUC but not AC while ALN differed from neither in most parameters. Connectivity density of the RIS group was significantly greater than all other groups, including AC at that time point.

After 56 days of recovery, Tb.N for AC (2.58 mm^{-1}) and HUC (2.8 mm^{-1}) was significantly lower than ALN (3.39 mm^{-1}) and RIS (3.45 mm^{-1}). The AC group (0.39 mm) had the highest mean Tb.Sp, which was significantly higher than ALN (0.29 mm) and RIS (0.28 mm). RIS again had the lowest Tb.Sp, but at day 112 it was significantly lower than both of the controls instead of only HUC. Conn. densities of the ALN (47.7 mm^{-3}) and RIS (53.8 mm^{-3}) groups were significantly greater than both AC (29.0 mm^{-3})

and HUC (30.9 mm^{-3}) but not different from each other. There were no significant differences in Tb.Th at day 112.

The AC group had the worst Tb.N, Tb.Sp, and connectivity density of all the groups at the end of recovery. This phenomenon likely due to the age-related decline in bone expected of 10 month old animals. At this time point too, both treatments provide favorable cancellous microarchitecture compared to the AC group. The BP groups' enhanced microarchitecture indicates that the treatments' effects persist into the recovery period. Or rather, that is true if the poorer microarchitecture of the AC group was due to age related losses.

Table 6: µCT Cancellous Densitometry Results

	BV/TV (%/100)	TMD (mg/cm^3)
Baseline		
AC	0.28 (0.07)	954.8 (31.9)
End of Pre-treatment (Day 28)		
AC	0.21 (0.02)	977.4 (11.6)
ALN	0.23 (0.04)	974.7 (15.8)
RIS	0.25 (0.05)	972.6 (13.0)
End of Hindlimb Unloading (Day 56)		
AC	0.21 (0.02)	974.6 (15.5)
HUC	0.15 (0.02) *	971.7 (21.5)
ALN	0.22 (0.03) †	979.5 (15.8)
RIS	0.26 (0.05) *†#	979.1 (17.5)
End of Recovery (Day 112)		
AC	0.18 (0.06)	1017.5 (37.3)
HUC	0.16 (0.04)	1009.2 (20)
ALN	0.20 (0.05)	987.8 (24.7)
RIS	0.23 (0.04) †	987.1 (19.4) †

Data presented as: Mean (Standard Deviation)
* - Significantly different from AC at $p < 0.05$
† - Significantly different from HUC at $p < 0.05$
# - Significant difference between treatments at $p < 0.05$
Italics indicates non-normal data assessed using Kruskal-Wallis with Dunn Post Hoc (Bonferroni Correction)
Red text indicates data which is non-normal and heteroscedastic

Table 7: µCT Cancellous Microarchitecture Results

Baseline	Trabecular Number (mm^{-1})	Trabecular Thickness (mm)	Trabecular Spacing (mm)	Connectivity Density (mm^{-3})	Degree of Anisotropy
AC	3.50 (0.42)	0.099 (0.011)	0.28 (0.04)	60.93 (12.63)	1.60 (0.07)
End of Pre-treatment (Day 28)					
AC	3.22 (0.30)	0.090 (0.003)	0.30 (0.03)	48.59 (9.89)	1.56 (0.07)
ALN	3.28 (0.54)	0.090 (0.003)	0.31 (0.05)	56.27 (13.32)	1.58 (0.06)
RIS	3.31 (0.48)	0.090 (0.006)	0.30 (0.05)	57.38 (12.51)	1.57 (0.03)
End of Hindlimb Unloading (Day 56)					
AC	3.27 (0.37)	0.090 (0.004)	0.30 (0.04)	49.71 (6.52)	1.51 (0.02)
HUC	2.95 (0.21)	0.080 (0.005) *	0.33 (0.03)	34.90 (9.27) *	1.52 (0.06)
ALN	3.28 (0.36)	0.090 (0.004) †	0.30 (0.05)	52.01 (6.68) †	1.55 (0.06)
RIS	3.58 (0.42) †	0.095 (0.007) †	0.27 (0.04) †	63.34 (12.69) *†#	1.58 (0.06) *
End of Recovery (Day 112)					
AC	2.58 (0.44)	0.110 (0.053)	0.39 (0.07)	28.97 (14.22)	1.50 (0.12)
HUC	2.80 (0.45)	0.090 (0.002)	0.35 (0.06)	30.94 (11.52)	1.47 (0.08)
ALN	3.39 (0.5) *†	0.090 (0.006)	0.29 (0.05) *	47.66 (16.52) *†	1.53 (0.04)
RIS	3.45 (0.48) *†	0.090 (0.003)	0.28 (0.06) *†	53.8 (14.3) *†	1.53 (0.05)

Data presented as: Mean (Standard Deviation)
* - Significantly different from AC at $p < 0.05$
† - Significantly different from HUC at $p < 0.05$
# - Significant difference between treatments at $p < 0.05$
Italics indicates non-normal data assessed using Kruskal-Wallis with Dunn Post Hoc (Bonferroni Correction)
Red text indicates data which is non-normal and heteroscedastic

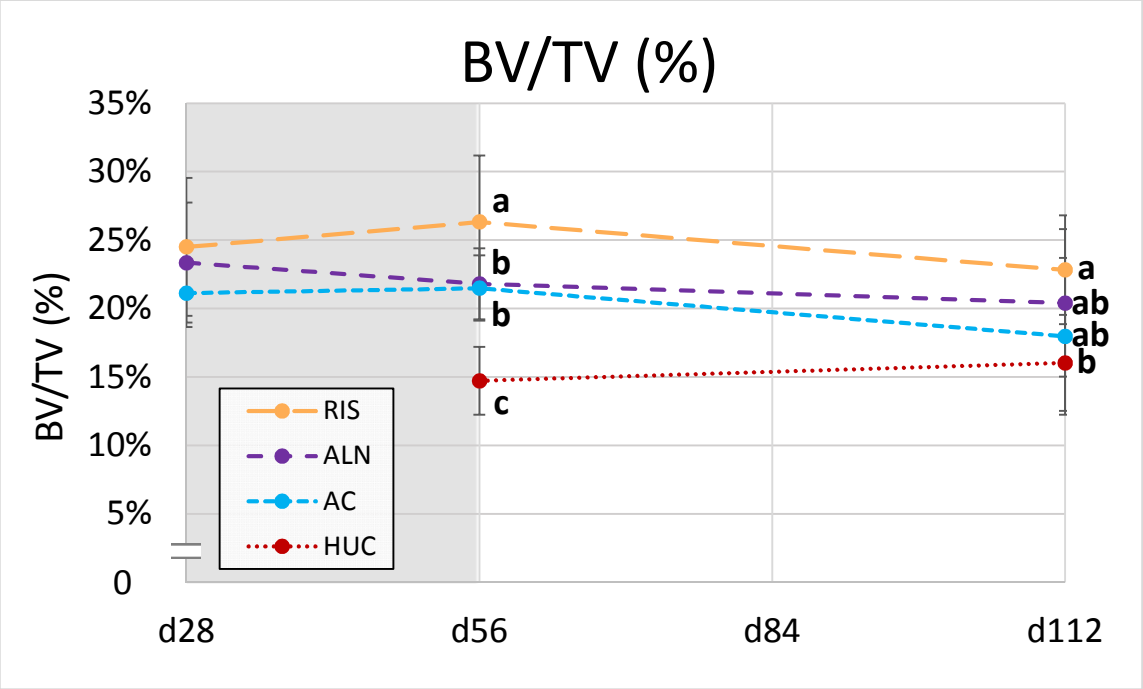

Figure 20: *Ex Vivo* µCT % Bone Volume per Total Volume of Distal Femur Metaphysis

Hindlimb unloading period is denoted by gray rectangle. Groups not sharing a letter are significantly different from each other. Data are presented as mean ± standard deviation.

At day 56, HUC had the lowest %BV/TV, which was significantly lower than AC and both treatment groups. RIS also had significantly higher %BV/TV than AC and ALN which is a direct difference between treatments. Both treatments protect from HU losses but RIS actually enhanced cancellous %BV/TV compared to AC. After recovery, RIS was still significantly greater than HUC but was no longer significantly different from AC or ALN. ALN and AC were n.s. different from HU controls.

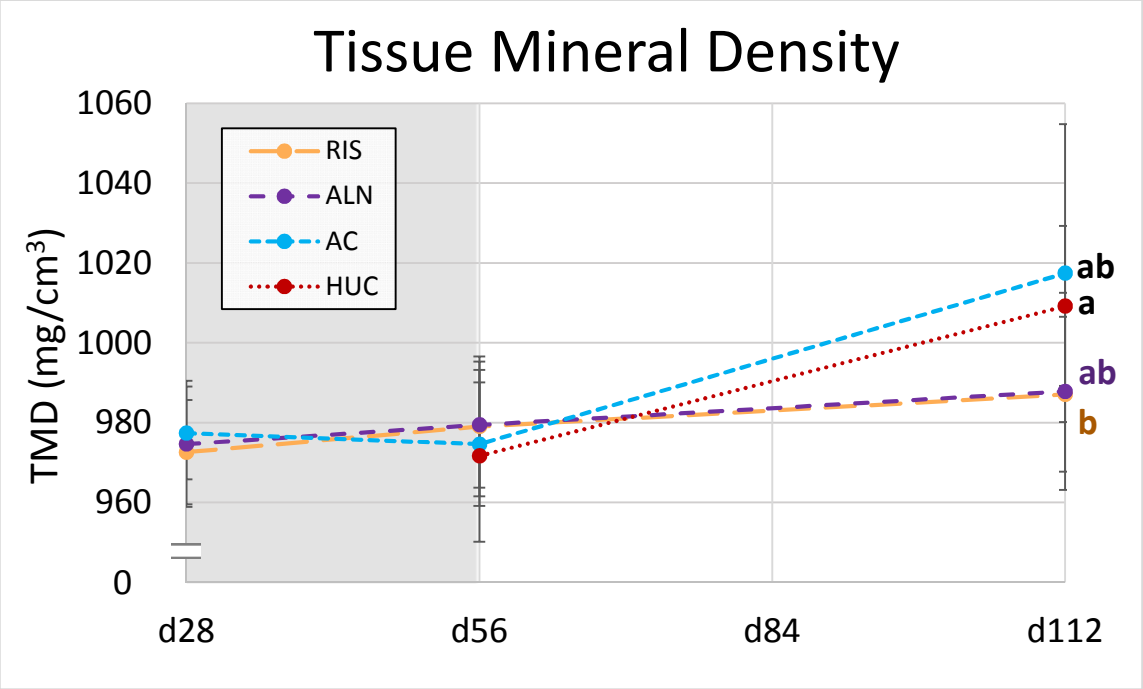

Figure 21: ***Ex Vivo*** **µCT Tissue Mineral Density of Distal Femur Metaphysis**

Hindlimb unloading period is denoted by gray rectangle. Groups not sharing a letter are significantly different from each other. Data are presented as mean ± standard deviation.

At day 56 there were no differences in tissue mineral density and this is consistent with cortical vBMD. By the end of recovery, the treatment groups are lowest thought ALN is n.s. lower than the control groups. The control group's higher averages are likely due to experiencing greater turnover than the treatment groups resulting in higher mineralization.

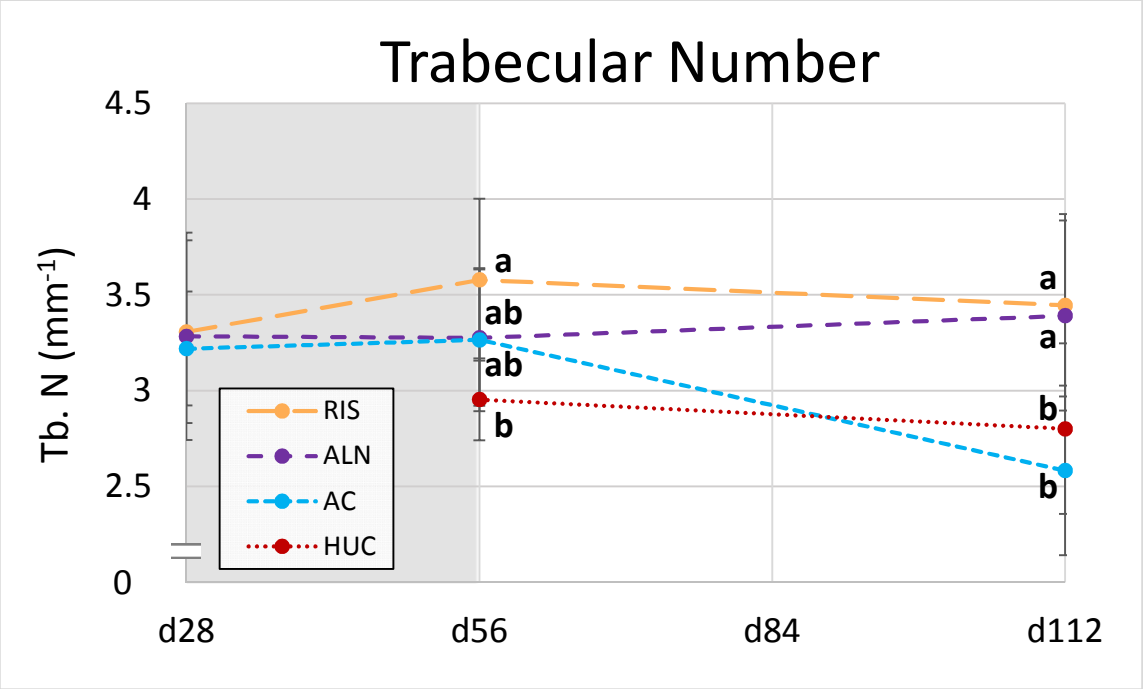

Figure 22: *Ex Vivo* µCT Trabecular Number of Distal Femur Metaphysis

Hindlimb unloading period is denoted by gray rectangle. Groups not sharing a letter are significantly different from each other. Data are presented as mean ± standard deviation.

At day 56, HUC did not have significantly lower Tb. N than AC but was significantly lower than RIS. RIS did not differ from ALN or AC so there was no direct difference between drug groups but there is the indirect one of relationship to HUC. At day 112, both controls are significantly lower than both treatments. This also is a parameter where there are suggestions of age related decline since AC ends up lower than any other group though n.s. from HUC. Both drugs appear to persist and protect trabecular number into recovery.

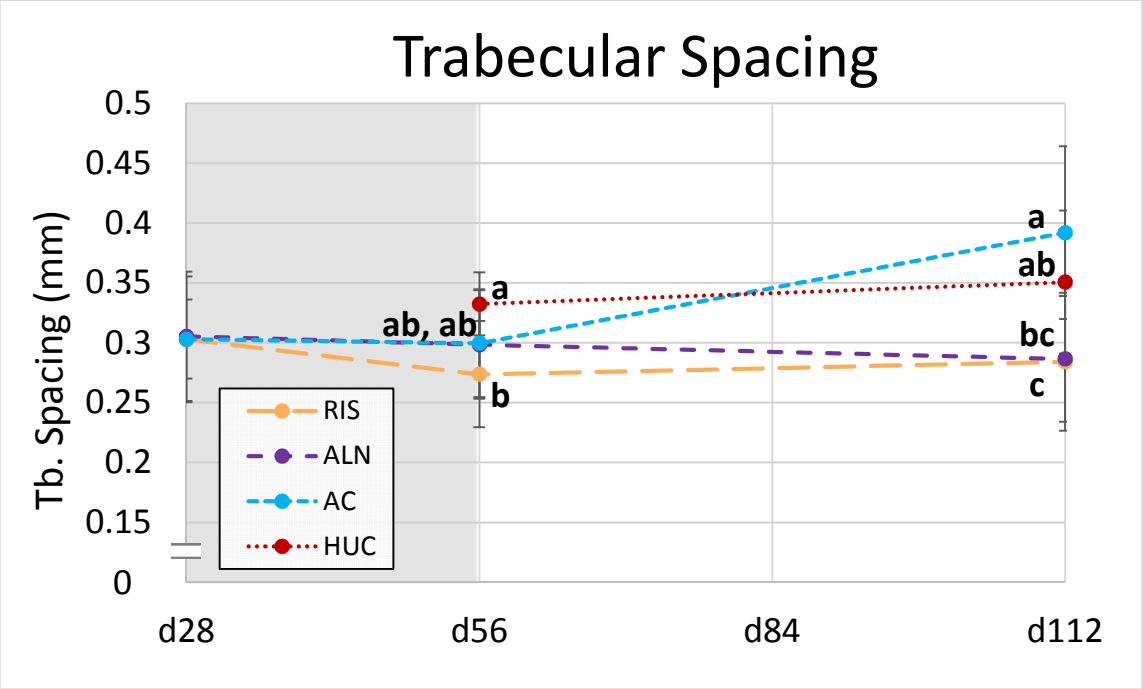

Figure 23: *Ex Vivo* µCT Trabecular Spacing of Distal Femur Metaphysis

Hindlimb unloading period is denoted by gray rectangle. Groups not sharing a letter are significantly different from each other. Data are presented as mean ± standard deviation.

It should be noted that having a lower value is preferable in trabecular spacing. Spacing at day 56 is lowest for RIS which is significantly lower than HUC. AC and ALN were not significantly different from HUC or RIS. At day 112, RIS again has lowest spacing which is significantly lower than HUC or AC but not ALN. ALN was not different from HUC or RIS but was significantly lower than AC. Again, there are hints of an age-related decline as AC has the highest spacing.

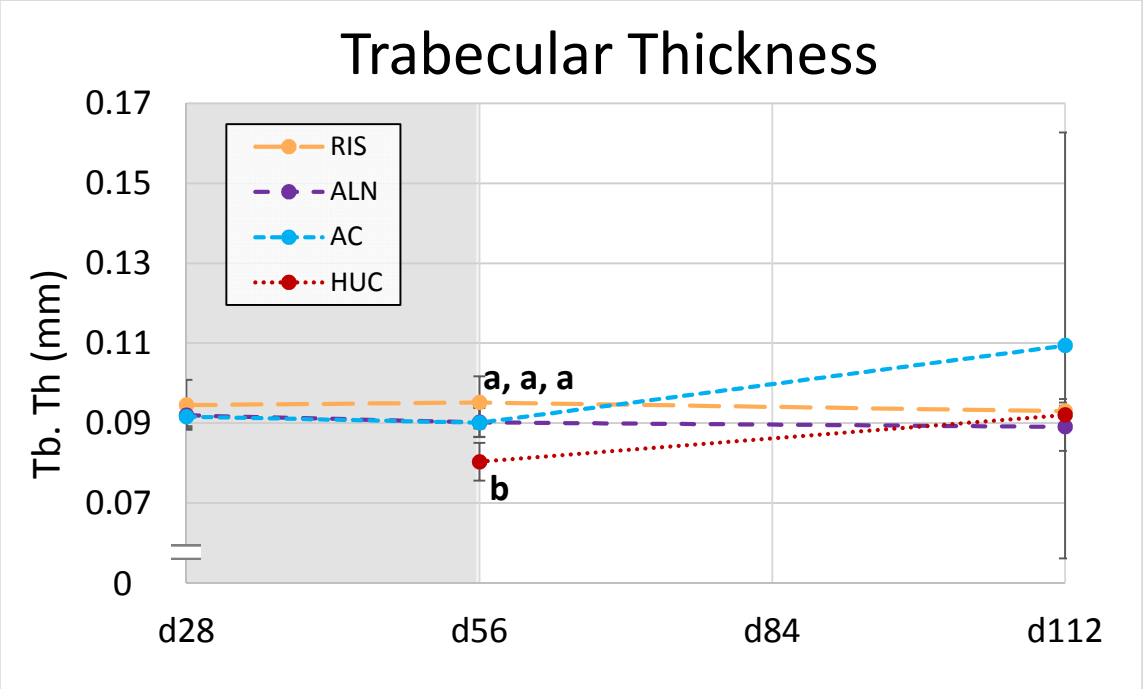

Figure 24: *Ex Vivo* µCT Trabecular Thickness of Distal Femur Metaphysis

Hindlimb unloading period is denoted by gray rectangle. Groups not sharing a letter are significantly different from each other. Data are presented as mean ± standard deviation.

At day 56, HUC had significantly lower trabecular thickness than AC and both of the treatment groups. BPs protected the trabecular thickness though the differences are rather small. At the end of recovery, there were no significant differences between groups though AC trended higher.

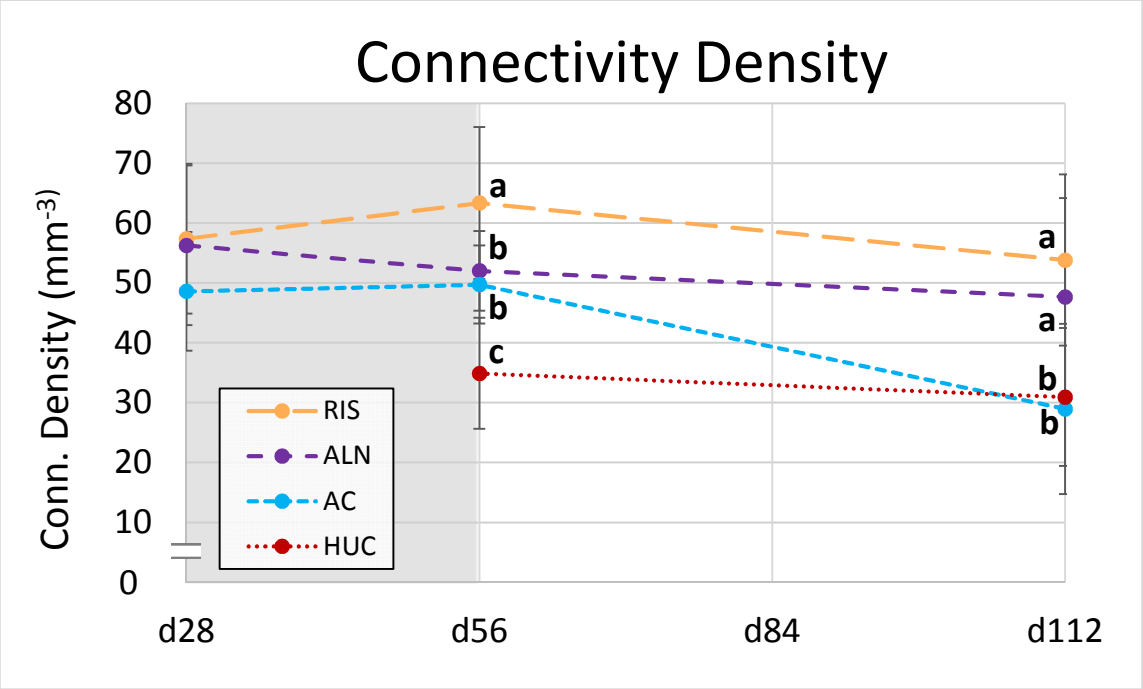

Figure 25: *Ex Vivo* µCT Connectivity Density of Distal Femur Metaphysis

Hindlimb unloading period is denoted by gray rectangle. Groups not sharing a letter are significantly different from each other. Data are presented as mean ± standard deviation.

At day 56, HUC has the lowest conn. density which does show unloading related decline since it is significantly lower than AC. RIS had significantly greater conn. density than ALN, AC, and HUC which reinforces the enhanced trabecular properties RIS yields. After recovery, both controls are significantly lower than both treatment groups. Again, the treatments persist into the recovery period when they are aging.

4.2 Reduced Platen Compression (RPC) Results

The lack of between-group differences at day 28 in all scanned parameters (both pQCT and μCT) meant that RPC data from this time point was excluded. The number of specimens tested does not match the number of bones originally collected. This was due to specimen loss and to specimens fracturing during the sectioning process. The number of bones used for RPC testing has been summarized in Table 8.

Table 8: Specimens Available for RPC Testing per Group at Each Time Point

	Day 56	Day 112
AC	6	6
HUC	8	10
ALN	11	12
RIS	10	15

Data tended to fail normality tests but passed an equality of variances test robust to non-normality. This means all significant differences presented indicate some group stochastically dominates (i.e., tends to have higher randomly chosen observations) than other groups do. The results do not mean that they have different means as that is not what a Kruskal-Wallis nor Dunn's test tests for. Further comparisons are performed with a Dunn Post Hoc test. All RPC data collected at the DFM are organized by group and time point in Table 9. The figures of all parameters with significant differences between groups for at least one time point appear below the text in order of mention.

4.2.1 Extrinsic Values

HU controls had the lowest average cancellous stiffness (25.4 N/mm) (Figure 26) at day 56, but were significantly lower only versus RIS (79.2 N/mm). At the end of recovery, the RIS and ALN groups (61.1 and 52.1 N/mm, respectively) had significantly higher average cancellous stiffness than AC (15.9 N/mm). Both drugs maintained stiffness that was not different from AC after the HU period. RIS does perform slightly better as it is significantly different from HUC after unloading, whereas ALN is not. BPs seem to protect against the presumed age-related decline of the AC group at day 112.

Average maximum force (Figure 27) at day 56 was 8.91 N for the RIS group which differed significantly from the HUC group's 2.70 N. At the end of recovery, RIS (7.32 N) had significantly higher maximum force than AC (2.36 N). RIS had greater average max force than the lowest groups at each time point (HUC at d56, AC at d112), which agrees with stiffness results. ALN was not significantly higher than ambulatory controls at day 112 in this parameter, which is different from stiffness results.

4.2.2 Estimated Intrinsic Properties

The estimated elastic modulus results (Figure 28) show the same trends in between-group differences as stiffness did, with slight differences in order. At day 56, AC had the second rather than third highest modulus, though it was not significantly different from ALN. There were no significant differences between the drug groups, but RIS was slightly better as it was both not different from AC and significantly greater than HUC. Both RIS (29.5 MPa) and ALN (25.2 MPa) had significantly higher elastic modulus than AC (8.2 MPa) at the end of recovery.

Average ultimate stress (Figure 29) showed a different trend at day 56 from the other mechanical parameters. ALN (1.68 MPa) and RIS (2.10 MPa) had significantly greater ultimate stress than the HUC (0.65 MPa) at day 56. At the end of recovery, ALN (1.4 MPa) and RIS (1.8 MPa) had higher ultimate stress than AC (0.60 MPa). The geometry used to obtain intrinsic properties influenced modulus minimally, but did affect between-group differences in ultimate stress. RIS and ALN did not differ significantly in ultimate stress at either time point, but RIS was n.s. higher at both.

Neither treatment differs from AC in either modulus or ultimate stress following unloading (day 56). HUC was not significantly lower than AC in both properties at day 56, but it did trend lower. RIS again appears indirectly superior to ALN, particularly in the elastic modulus after unloading. RIS was indirectly superior in that elastic modulus was significantly higher than HUC while ALN did not differ from HUC. AC also shows further indications of aging bone with lower elastic modulus and ultimate stress than both treatments at the end of recovery.

Table 9: RPC Estimated Cancellous Mechanical Properties

	Stiffness (N/mm)	Max Force (N)	Yield Force (N)	Yield Stress (MPa)	Modulus (MPa)	Ultimate Stress (MPa)
End of Hindlimb Unloading (Day 56)						
AC	*58.8 (62.9)*	*6.71 (5.35)*	*5.24 (4.36)*	1.40 (1.09)	*28.7 (24.9)*	*1.78 (1.25)*
HUC	*25.4 (30.5)*	*2.70 (2.69)*	*2.38 (2.66)*	0.57 (0.49)	*11.4 (9.3)*	*0.65 (0.49)*
ALN	*66.3 (51.6)*	*7.18 (4.89)*	*5.69 (3.46)*	1.35 (0.69)	*28.6 (19.4)*	*1.68 (0.93) †*
RIS	*79.2 (31.9) †*	*8.91 (3.89) †*	*7.79 (3.02) †*	1.84 (0.67) †	*35.2 (14.6) †*	*2.10 (0.88) †*
End of Recovery (Day 112)						
AC	*15.9 (10.5)*	*2.36 (1.51)*	*2.13 (1.35)*	0.54 (0.33)	*8.2 (5.3)*	*0.60 (0.36)*
HUC	*37.1 (32.4)*	*4.02 (3.26)*	*2.97 (1.79)*	0.75 (0.48)	*17.3 (15.6)*	*0.99 (0.83)*
ALN	*52.1 (34.0) **	*6.05 (3.45)*	*4.74 (2.31)*	1.12 (0.51)	*25.2 (17.8) **	*1.40 (0.67) **
RIS	*61.1 (41.6) **	*7.32 (4.85) **	*6.02 (4.65) **	1.47 (1.08)	*29.5 (18.6) **	*1.80 (1.1) **

Data presented as: Mean (Standard Deviation)
* - Significantly different from AC at $p < 0.05$
† - Significantly different from HUC at $p < 0.05$
# - Significant difference between treatments at $p < 0.05$
Italics indicates non-normal data assessed using Kruskal-Wallis with Dunn Post Hoc (Bonferroni Correction)
Red text indicates data which is non-normal and heteroscedastic

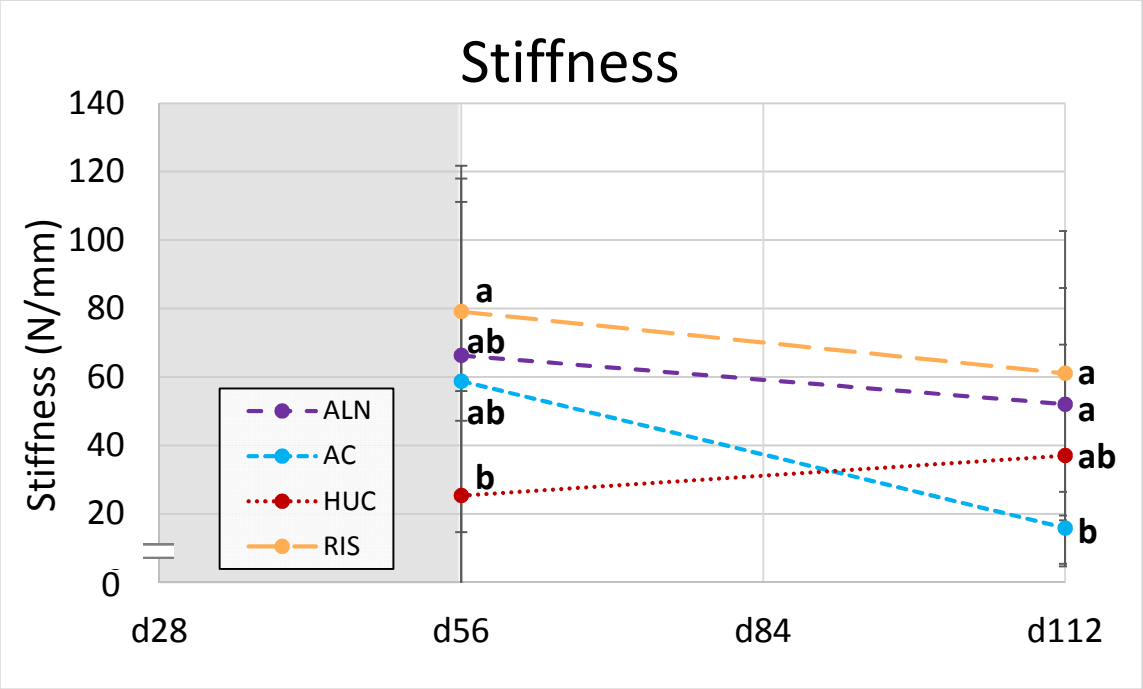

Figure 26: *Ex Vivo* RPC Estimated Stiffness of Distal Femur Metaphysis

Hindlimb unloading period is denoted by gray rectangle. Groups not sharing a letter are significantly different from each other. Data are presented as mean ± standard deviation.

At day 56, HUC is not significantly lower than AC or ALN which indicates HU did not significantly reduce stiffness for HU controls. RIS had significantly greater cancellous stiffness than HUC. After recovery, AC is the least stiff though it is not significantly lower from HUC. Both treatment groups are significantly stiffer than AC which would indicate a persisting treatment effects.

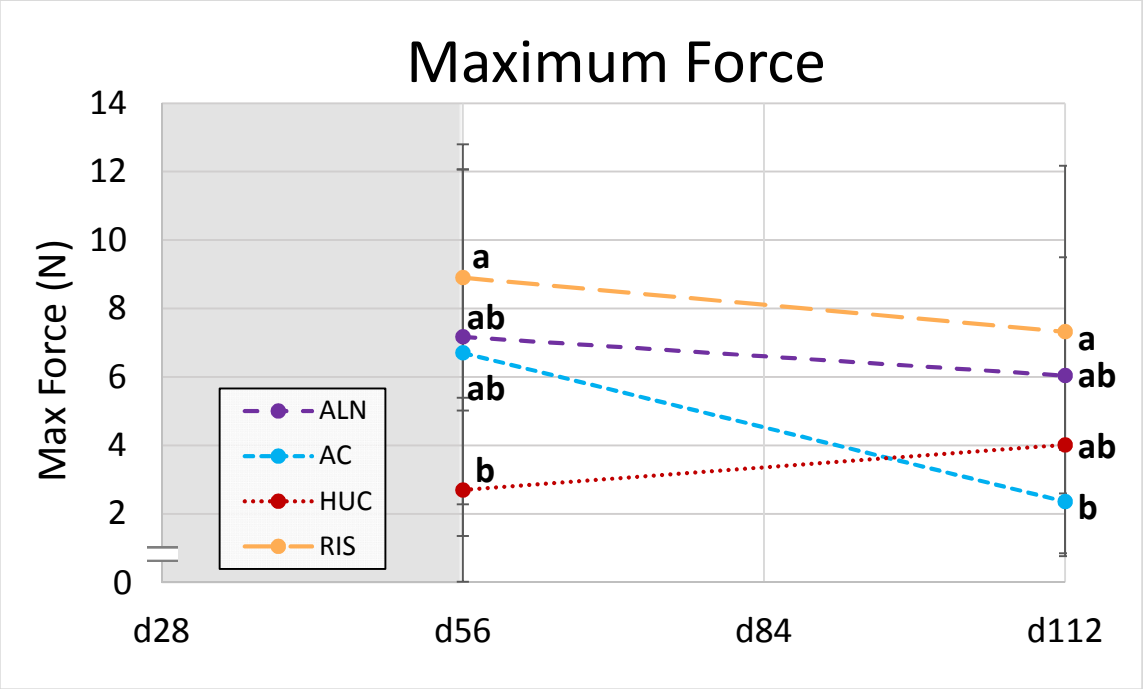

Figure 27: *Ex Vivo* RPC Maximum Force of Distal Femur Metaphysis

Hindlimb unloading period is denoted by gray rectangle. Groups not sharing a letter are significantly different from each other. Data are presented as mean ± standard deviation.

The between-group differences at day 56 match those seen in stiffness but differ at day 112. At the end of recovery, the RIS group's maximum force is the only one significantly greater than AC. This is another instance of RIS slightly outperforming ALN though it is notable that here it is in a mechanical parameter.

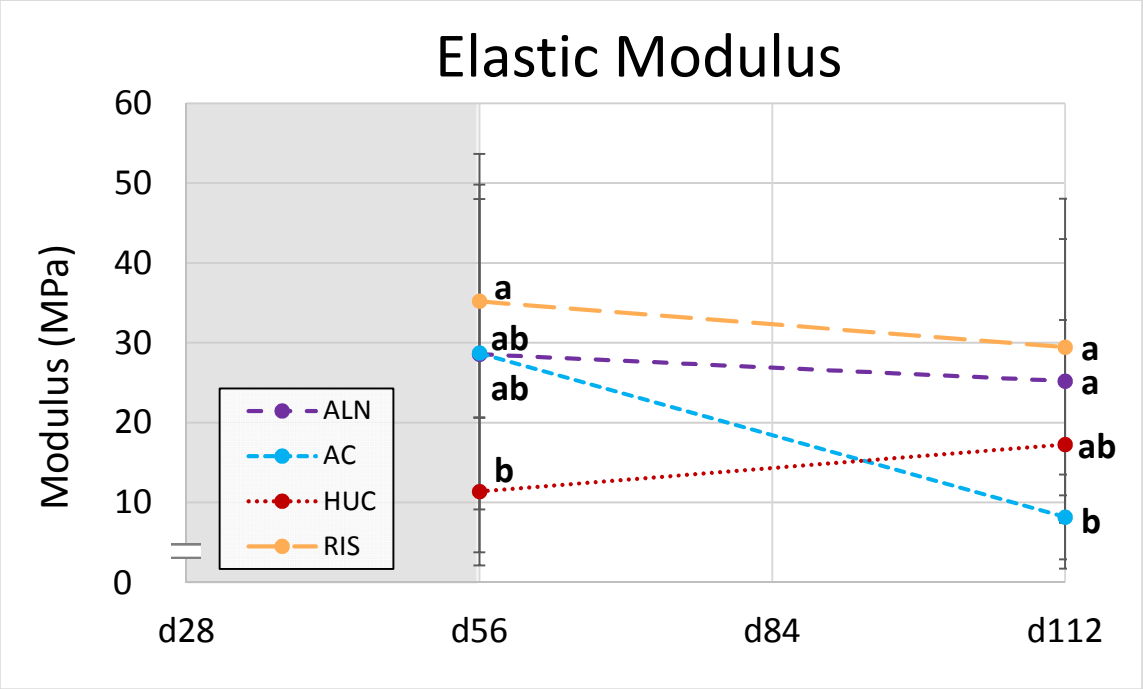

Figure 28: *Ex Vivo* RPC Elastic Modulus of Distal Femur Metaphysis

Hindlimb unloading period is denoted by gray rectangle. Groups not sharing a letter are significantly different from each other. Data are presented as mean ± standard deviation.

The overall trends and between-group differences of elastic modulus match those seen in stiffness at both time points. RIS protected from n.s. unloading losses and both RIS and ALN protected from possible age-related decline of the AC group.

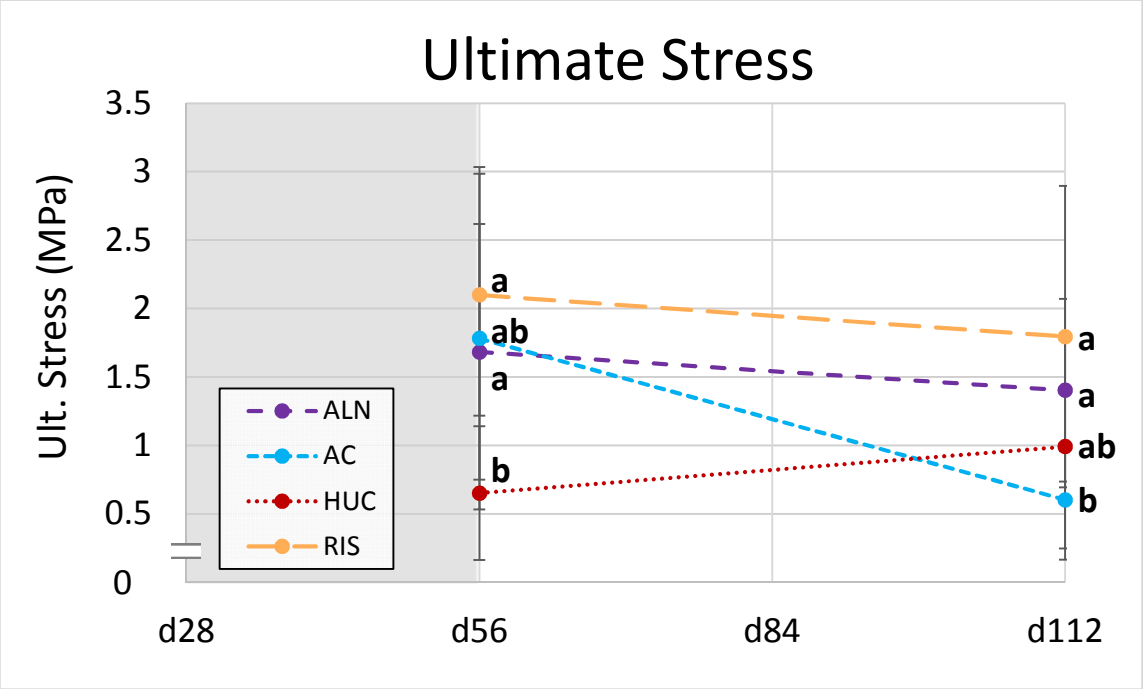

Figure 29: *Ex Vivo* RPC Ultimate Stress of Distal Femur Metaphysis

Hindlimb unloading period is denoted by gray rectangle. Groups not sharing a letter are significantly different from each other. Data are presented as mean ± standard deviation.

At day 56, both RIS and ALN had significantly higher ultimate stress than HUC. At day 112, both treatments had significantly higher ultimate stress than AC. Both treatments seem to prevent the n.s. losses of HUC and prevent the possible age-related decline of AC at day 112.

5. DISCUSSION

For pQCT results, the HUC group had significantly lower average total BMC, total vBMD, cancellous vBMD, cortical BMC, and cortical thickness than ambulatory controls after HU. In all these parameters both treatments groups had significantly higher average values than HUC. This indicates protection on the part of both risedronate and alendronate. At the end of recovery, there were no significant differences between the two control groups in either densitometry or geometry. Risedronate seemed to be best for the cancellous region and overall total cross-section at day 112, but was lowest in a number of cortical parameters and significantly worse in cortical vBMD than ambulatory controls. Both drugs effectively protected cancellous bone densitometry and geometry at both days 56 and 112. Alendronate seemed to persist longer in the cortical region than RIS did. The ALN group values were not significantly different from ambulatory controls in cortical vBMD at the end of recovery but RIS values were lower than AC.

Micro CT data indicate that both drugs protect the cancellous region from hindlimb unloading related losses in BV/TV, trabecular thickness, and connectivity density. Risedronate again seems to perform slightly better than alendronate despite there only being two direct significant differences between them, which were in BV/TV and connectivity density at day 56. For other μCT variables, RIS trended toward enhanced microarchitectural characteristics compared to all other groups. In many cases, the RIS group's parameter average was significantly better than HU controls at day 56 and ambulatory controls at day 112. ALN maintained properties comparable to the best control group at each time point, which was the AC group at day 56 and the HUC group at day 112. Generally, while ALN was not different from the best control, it was also not different from the worse control group.

Results from μCT provide insight into the way bone is resorbed in the cancellous region. At both day 56 (end of HU) and day 112 (end of recovery), there is a loss in bone quality as qualified by decreases in multiple parameters (connectivity density, Tb.N, Tb.Th) or increases in trabecular spacing. The only significant differences in trabecular

thickness were at day 56 (end of HU) where the HUC group was lower than the three other groups. In contrast, other parameters showed more between-group differences. Trabecular number was not significantly lower for the HUC group compared to AC after unloading, but connectivity density was. This suggests that the non-significant reduction in trabecular number affected connectivity and thickness during unloading without significantly affecting overall spacing. Connectivity density was protected by both BPs, which suggests the drug distribution in the cancellous bone is relatively even.

The way cancellous bone is resorbed differed during the recovery period. At the end of recovery, there were no significant differences in trabecular thickness between groups. However, both treatment groups had significantly greater trabecular number and connectivity density than both controls. This suggests that, during recovery, trabecular thickness is not reduced uniformly during resorption. Instead, as both control groups aged with normal ambulation, trabeculae are completely resorbed and connectivity is reduced. These reductions are paired with increases in spacing that would contribute to a worse overall structure. This deterioration is most severe in the ambulatory controls, which makes it seem unlikely that HU controls would fully recover cancellous bone quality given longer recovery.

The trends seen in the trabecular architecture μCT data correspond well with those seen in the RPC data. In both data sets, there is an indication that risedronate has a slight advantage over alendronate but that both are effective and seem to last into the recovery period. The notable exception was in the RIS group and for cortical vBMD, which was significantly lower at the end of recovery. It was previously hypothesized that risedronate with its lower binding affinity would bind preferentially to the higher surface area cancellous region. The fact that the RIS group experienced persistent benefits through recovery in the cancellous region but not in the cortical region is consistent with this notion. Poorer binding to cortical bone limits the length of time risedronate can be considered effective in protecting bone as a whole (cortical and cancellous).

Stiffness, elastic modulus, maximum force, and ultimate stress show between-group differences and trends most similar to trabecular number. The between-group

differences at each time point for each of the four mechanical parameters are not quite the same. The primary difference is in the HU controls at day 112. Trabecular number at day 112 was significantly lower for both control groups as compared to both treatment groups. HUC group stiffness, modulus, and ultimate stress at day 112 was neither different from ambulatory controls nor treatment groups. The second difference was that the ALN group had ultimate stress that significantly differed from the HUC group at day 56. Neither trabecular number nor any of the other mechanical parameters showed this difference. Compared to μCT data, there were fewer differences between groups for the RPC data. Part of that is likely due to many RPC parameters having far greater proportional variance compared to the μCT data parameters, and due to the limitations noted in the background. It could also be that cancellous mechanical parameters are not affected to the same extent by changes to architecture.

The difference in the extent of the effect can be seen in the disparity in between-group percent differences for mechanical parameters versus CT parameters. After unloading (day 56), RIS had significantly higher modulus (102.3% diff.) and ultimate stress (105.3% diff.) than HUC. RIS also had significantly higher Tb.N than HUC at day 56, but the percent difference was only 19.1%. Similarly, RIS had significantly higher cancellous vBMD than HUC at day 56 but this percent difference was 31.7%. The μCT parameter with the greatest percent difference between RIS and HUC at that day 56 was connectivity density and it was only 57.9% different. These percent differences for an AC and HUC comparison of modulus and ultimate stress at day 56 were similarly large at 86.4% and 92.9%, respectively. For this pair of groups the largest percent difference in a μCT parameter was in BV/TV, which had a 37.4% difference. The percent difference between AC and HUC in cancellous vBMD was 19.0%. The proportions formed by comparing those pairs of CT and mechanical parameter percent differences are different for day 56 and day 112. Changes in trabecular architecture did not produce consistently proportionate changes in mechanical properties. This only serves to reinforce the fact that, at least in the cancellous region, mechanical performance is not fully explained by densitometry or architecture.

One recurring characteristic across most results was the risedronate group being either indirectly better or directly better than the alendronate group. As explained previously, a direct difference is like risedronate being significantly different from alendronate in a particular outcome variable. An indirect difference would be if the risedronate group was significantly different from HUC after unloading, while the alendronate group was not significantly different from HUC. This was the case for modulus, stiffness, max force, trabecular number, degree of anisotropy, and cancellous vBMD. After recovery, this pattern appeared in BV/TV and cancellous vBMD. There were direct differences between the treatments after unloading with RIS having significantly greater BV/TV and connectivity density than ALN. Risedronate protected the cancellous region's densitometry, geometry, and mechanical performance through unloading and recovery. In the cortical region though, there did seem to be a loss in efficacy by the end of recovery. The RIS group had the lowest (non-significant) area, thickness, and bone mineral content in the cortical region and significantly lower cortical vBMD than ambulatory controls.

Another recurring trend was the AC group values being non-significantly lower than HUC and significantly lower than at least one BP treatment group at the end of recovery. This was the case for both ultimate stress and modulus. It was also seen in trabecular number, connectivity density, cancellous BMC, and cancellous vBMD. In contrast, ambulatory controls trended higher at the end of recovery than the other groups in total vBMD, cortical BMC, and cortical vBMD. The argument could be made that the HU, RIS, and ALN groups have greater amounts cancellous bone (BMC) because resorption of the inner face of the cortex has increased porosity to the point that it resembles cancellous bone. However, that explanation is problematic considering the AC group's cancellous vBMD is significantly lower than that of the BP treatment groups. Lower cancellous mineral density would suggest increased turnover was occurring in the cancellous bone of the AC group. Estimated elastic modulus and ultimate stress for the AC group are also significantly lower than those of the BP-treated groups. Ultimate stress and elastic modulus are intrinsic properties meaning that these

properties are independent of bone mass. In addition, the platen would mostly avoid any recently trabecularized bone since the platen is sized as 70% of the area of the largest circle that can be inscribed.

Risedronate slightly outperforming alendronate in most parameters, but specifically in the cancellous region, is unsurprising based on earlier hypotheses. However, it is difficult to compare these findings to other studies. Few studies have examined both the resulting mechanical and densitometric (cortical, cancellous, and or total bone) parameter differences between these two drugs in the past. A study by Allen et al. did include both types of measures but they used intact beagles who were not in a state of increased resorption [29]. In one human osteoporosis study by Reid et al., risedronate treatment yielded inferior increases in trochanter BMD (1.5% difference) and at other sites as compared to alendronate [30]. They also found that alendronate reduced bone turnover markers more compared to risedronate. However, another human osteoporosis study by Silverman et al. showed risedronate was superior in reducing hip and non-vertebral fracture rates as compared to alendronate [31]. This last study had similar findings to those in the current thesis experiment with respect to mechanical performance. The findings of this thesis that treatment with risedronate yielded better (though non-significant) mechanical properties compared to alendronate compare favorably with the results reported by Silverman et al. [31].

Alendronate's efficacy in preventing losses from disuse in humans has been evaluated using bed rest studies. In one study by Leblanc et al., alendronate was administered concurrently with a 17-week long bed rest period [32]. Subjects who were not treated saw significant losses from baseline in BMD at the lumbar spine, femoral neck, and trochanter. The alendronate-treated group did not experience significant losses compared to baseline at any of these three sites. In fact, the alendronate-treated group saw a significant increase in BMD compared to baseline at the femoral neck. The alendronate group also had significantly higher BMD than controls at all three sites. These data agree with the findings of this experiment that alendronate was effective. Leblanc et al. also studied the combined effects of alendronate (ALN) treatment with

aRED exercise in astronauts during 5.5 months on the ISS [5]. Subjects who just exercised with aRED, but did not take ALN, did not experience significant loses in DEXA BMD at the femoral neck, lumbar spine, pelvis, or trochanter. However, they did incur losses in total hip BMD. The ALN+aRED group did not experience significant losses in BMD at any of those five sites. This group also had significantly higher BMD than the aRED exercise group in the total hip and lumbar spine. The ALN+aRED group also had significantly higher BMD than the non-aRED group at all sites. QCT scans of the femoral neck, trochanter, and total hip showed that the ALN+aRED group had no significant pre-post losses in cortical, cancellous, and total vBMD. Their findings agree with the protection alendronate provided for DFM cortical, cancellous, and total vBMD at the end of unloading in the current experiment.

Previous animal studies have examined alendronate's efficacy in preventing HU losses in rats when administered concurrently with unloading. One study, by Swift et al. found that administration of ALN prevented losses from the beginning to the end of an HU period in total vBMD and cancellous vBMD at the proximal tibia metaphysis (PTM) [33]. However, they also found that concurrent ALN treatment mitigated rather than protected against losses in total BMC. In the cancellous region, ALN treatment yielded %BV/TV that was significantly lower than that of ambulatory controls and Tb.Th that was significantly lower than that of ambulatory and HU controls [33]. These results are at a different bone site (PTM) than that examined in this experiment (DFM). However, it appears that alendronate may perform better as a pre-treatment since these significant losses were not observed at the DFM in this experiment. There was not a similar rat hindlimb unloading study that administered risedronate concurrently with HU. However, Mosekilde et al. did administer both risedronate and alendronate to female rats using a hindlimb immobilization model for disuse [34]. They found a dose dependence in the response, but the two higher doses of both risedronate (0.2 and 1.0 mg/kg BW/day) and alendronate (1.0 and 2.0 mg/kg BW/day) prevented the losses in DEXA BMD experienced by the immobilized controls.

In the study by Mosekilde et al., the DFM was also mechanically tested by compression, and they reported a dose-dependent response [34]. Specifically, they found that the lowest dose of risedronate did not protect average maximum force against the losses seen in immobilized controls. The bones of animals treated with either of the two higher doses of risedronate or the highest dose of alendronate broke at a significantly higher force than immobilized controls [34]. Notably, treatment with either of the two lower doses of alendronate yielded DFM samples that broke at an average force that differed neither from immobilized nor normal controls. The findings of their middle and highest doses of these drugs are comparable to the between-group differences observed in the current experiment at the end of HU. They were however able to demonstrate differences between their ambulatory and non-treated controls that were not present in the current experiment.

Two studies by Fuchs et al. also examined the mechanical properties of ovariectomized (OVX) rats treated with either alendronate or risedronate. In the first of the two, they compressed the L4 vertebra, another mixed bone site, of alendronate-treated rats [35]. They did not find any significant differences in stiffness, ultimate force, ultimate stress, or modulus between their non-OVX controls and their OVX controls. Similarly, they did not find any difference between the OVX-ALN group and either control group. In the second study, OVX rats were administered either alendronate (2.4 μg/kg BW 3x/week), a lowdose of risedronate (1.2 μg/kg BW 3x/week), or a high dose of risedronate (2.4 μg/kg BW 3x/week) for eight weeks [36]. At the end of the 8 week period, there were no significant differences in the same four mechanical parameters examined in their previous studies for the lumbar spine. After withdrawal, they continued to monitor these parameters and found that 12 weeks after withdrawal the modulus of the high dose risedronate group was siginificantly higher than OVX controls. The ultimate stress of the ALN group was greater than OVX controls 4 weeks after withdrawal. Treatment with the high dose of risedronate also resulted in ultimate stress that was significantly higher than OVX controls 12 weeks after withdrawal. They did not find direct differences between the BP treatment groups and found there were no

differences in modulus and ultimate stress 16 weeks after withdrawal. This is quite different from the findings of the current experiment where the positive effects of BPs on mechanical properties persisted for a withdrawal period three times the length of the treatment period (but only 12 weeks in absolute terms). In their study though, the increased resorptive state lasted for the entirety of the study. In general, other studies did not see the enhancement of mechanical properties that the alendronate and risedronate treatment groups demonstrated in this experiment.

The second Fuchs et al. study focused on the persistence of the BP effects after withdrawal. Their mechanical testing findings have already been mentioned; however, their histology findings are of interest as well. At the end of treatment, they found that osteoclast number normalized by bone surface (Oc.N/BS) was significantly lower for all BP-treated groups compared to OVX controls in the PTM [36]. This would indicate that all BP-treated groups experience decreased resorption compared to OVX controls by the end of treatment. After 16 weeks of withdrawal, there were no differences between the groups in the PTM. In the lumbar spine, the group treated with the low dose of risedronate had significantly higher (Oc.N/BS) after 12 and 16 weeks of withdrawal. They also found that bone formation rate was suppressed at the PTM for all BP-treated groups until 4 weeks after withdrawal. At 12 and 16 weeks after withdrawal, the alendronate group continued to have suppressed formation. Both risedronate groups had bone formation rates that did not differ from OVX controls. Their findings do not quite correspond to the length the positive effects of BPs persisted in the current experiment. In the current study, the ALN and RIS groups had significantly higher total vBMD than HUC 12 weeks after withdrawal. Again, 12 weeks for the current experiment is three times the length of the 4-week treatment period. Additionally, the RIS group had significantly higher cancellous vBMD than ambulatory controls 12 weeks after withdrawal. However, they do agree with the indications that risedronate persists for a shorter time than does alendronate.

6. LIMITATIONS

There were limitations to this experiment that must be acknowledged. This experiment used an animal model to simulate the microgravity exposure that astronauts experience. While this study used only male rats, the astronaut population of interest would include both males and females which do have different bone considerations. This thesis also only covers the results at the DFM, which is not the only mixed skeletal site and may not be the one whose response is most like the response of the human femoral neck. Additionally, the lower number of animals for both the ambulatory and HU control groups limited the statistical power for familywise comparisons. This was particularly harmful to the RPC analysis as those data had greater relative variance than pQCT and μCT data.

Another limitation was in the experimental design which did not include BP pre-treated groups that were not hindlimb unloaded. Due to this, the HUC group was the only group at the end of HU that could be said to have experienced losses due to HU despite the *ex vivo* nature of the data. This is because it was the only group with an appropriate age matched ambulatory control. Differences in the average value of parameters for BP-treated groups compared to ambulatory controls after unloading cannot therefore be considered to be differences due to an HU effect alone.

The limitations in mechanical testing were mentioned in the background; however, they are worth reiterating. The accuracy of RPC testing results is limited by end effects, continuum limits, heterogeneity, and anisotropy. Estimates for mechanical properties are for the tested structures rather than a true measure of the properties of cancellous bone as an isolated material. Additionally, these intrinsic property estimates may be underestimates since the equations used to calculate them are based on an assumption that platen area is equal to the compressed area. Any regions of missing trabeculae would reduce the actual area the compressive force is applied to. This would mean the denominator in strength and modulus calculations would be smaller in those cases. However, DFM samples used in this experiment did not exhibit these regions of

significantly reduced trabeculae. Alternatively, the region of cancellous bone compressed during RPC testing is connected, though not immediately, to the surrounding cortical shell. This could lead to the test overestimating the mechanical response. These experimental imperfections are inherent to this method, and the properties found using this method must be considered estimates.

7. CONCLUSIONS

In this study, a rat hindlimb unloading model was used to examine the efficacy of a pre-treatment approach to administering BPs in preventing HU-related bone loss. Microgravity was only simulated but this experiment's results have high relevance to the skeletal health of current and future astronaut population. The aim was to gain a better understanding of how bisphosphonates of differing binding affinity and antiresorptive potency affect bone densitometry measures and cancellous mechanical properties. It was also important to see if a pre-treatment approach was feasible, compared to concurrent administration, because there are some side effects to taking bisphosphonates that would be more troublesome if experienced while in space.

Skeletally mature rats were separated into four groups, two of which received BP pre-treatment of either risedronate or alendronate for 28 days. The two treatment groups and hindlimb unloaded controls then underwent a 28-day period of HU. Finally, the three unloaded groups were reambulated for 56 days of recovery. At key time points in the study, animals were euthanized and femurs were harvested. The DFM was scanned with both pQCT and μCT to assess the effects of HU and BP efficacy in mitigating those effects. The cancellous region of DFM cross-sectional slices was subjected to reduced platen compression testing and the intrinsic mechanical properties estimated.

The distal femur metaphysis was chosen for this study, as its mixed cortical and cancellous composition is more similar to a human femoral neck than is a rat's femoral neck. Regardless, the findings presented above and conclusions drawn below are from rats and may not predict exactly what would happen to human bone.

There were four questions introduced in the objectives section that the data from this study were intended to answer. The primary question was whether BPs administered as pre-treatments effectively protect bone at the DFM from the effects of HU. Both BPs do protect bone densitometry and geometry from all deleterious effects of HU at the DFM, but there was an apparently superior treatment. Risedronate outperformed alendronate significantly, or nonsignificantly, in numerous parameters across pQCT,

μCT, and mechanical testing. In addition, risedronate was sometimes indirectly better, as the RIS group would differ from HU controls but not ambulatory controls, whereas alendronate differed from neither control group.

The next question was whether the BP efficacy would be bone-type (i.e. cancellous or cortical) dependent at the DFM. After unloading, both BPs are effective in both the cancellous and cortical region. However, at the end of recovery, risedronate performs worse in the cortical region than in the cancellous region. This observation is likely linked to the question of how a pre-treatment approach may affect the persistence of BP effects into recovery. Risedronate's lower binding affinity may have led to lesser binding in the cortical region compared to alendronate. By the end of recovery, risedronate's positive effects do not persist in the cortical region while alendronate's positive effects do. Conversely, both treatments appeared to remain effective in the cancellous region through the recovery period. This longer persistence of the BPs' positive effects in the cancellous bone might be attributable to a greater amount of BPs binding to cancellous bone due to its high surface area.

The final question was whether cancellous mechanical properties would correspond well with cancellous microarchitectural parameters. Trends are certainly similar between trabecular number and the estimated elastic modulus and ultimate stress. There are a few other μCT parameters that show similar trends and BV/TV and connectivity density are among them. However, μCT parameters generally showed more between-group differences than seen in mechanical properties. Both sets of data tend to show the BP-treated groups having enhanced parameters, whether architectural or mechanical, compared to those of ambulatory controls at the end of recovery. In trabecular architecture, however, BP treatment groups had significantly enhanced bone quality compared to both control groups at the end of recovery. There was a noticeable disagreement between RPC and μCT parameters in the magnitude of the effects of BP pre-treatment. Estimated mechanical properties had much larger, sometimes three times larger, percent differences between groups than those seen in μCT parameters.

Additionally, the disparities in the magnitudes of percent differences between groups were not consistent between time points.

Overall, the results presented clearly indicate that a pre-treatment approach with either BP is very feasible since reductions in efficacy only occurred at the end of recovery. This study was performed on rats and focuses on the DFM, but the larger study does include more bone sites. Literature on bisphosphonate treatment timelines agree that the administration can be done in advance, as is the case in monthly-dosed versus daily-dosed osteoporosis patients. It is reasonable to infer that a pre-treatment approach would likely be effective for astronauts as well.

For this study, risedronate was the superior treatment for cancellous bone at the DFM in both its ability to protect densitometry measures and mechanical performance. Cancellous bone is exceedingly important at mixed relevant bone sites, such as the human femoral neck and vertebra, and its ability to absorb energy is integral to preventing fracture. Risedronate would have been the clearly superior treatment if its effects in the cortical region had better persisted into recovery. Alendronate was the better treatment from a pre-treatment standpoint, as the treatment's effects persisted to the end of recovery. The effects of alendronate were not as strong as risedronate's for the entire bone cross-section (both cancellous core and cortical shell) at the end of unloading. However, alendronate's positive effects persisted into recovery in both cortical and cancellous bone. The final decision of which of these two qualities, strength or persistence in the total bone, is most important to astronaut skeletal health is best left to their physicians.

REFERENCES

[1] E. Morey-Holton, R.K. Globus, A. Kaplansky, G. Durnova, The hindlimb unloading rat model: literature overview, technique update and comparison with space flight data, Adv Space Biol Med, 10 (2005) 7-40.

[2] A. LeBlanc, V. Schneider, L. Shackelford, S. West, V. Oganov, A. Bakulin, L. Voronin, Bone mineral and lean tissue loss after long duration space flight, J Musculoskelet Neuronal Interact, 1 (2000) 157-160.

[3] M.T. Hannan, D.T. Felson, B. Dawson-Hughes, K.L. Tucker, L.A. Cupples, P.W. Wilson, D.P. Kiel, Risk factors for longitudinal bone loss in elderly men and women: the Framingham Osteoporosis Study, J Bone Miner Res, 15 (2000) 710-720.

[4] T. Lang, J.J.W.A. Van Loon, S. Bloomfield, L. Vico, A. Chopard, J. Rittweger, A. Kyparos, D. Blottner, I. Vuori, R. Gerzer, P.R. Cavanagh, Towards human exploration of space: the THESEUS review series on muscle and bone research priorities, npj Microgravity, 3 (2017) 8.

[5] A. Leblanc, T. Matsumoto, J. Jones, J. Shapiro, T. Lang et al., Bisphosphonates as a supplement to exercise to protect bone during long-duration spaceflight, Osteoporos Int, 24 (2013) 2105-2114.

[6] E.S. Siris, S. Baim, A. Nattiv, Primary care use of FRAX: absolute fracture risk assessment in postmenopausal women and older men, Postgrad Med, 122 (2010) 82-90.

[7] E.S. Siris, S.K. Brenneman, E. Barrett-Connor, P.D. Miller, S. Sajjan, M.L. Berger, Y.T. Chen, The effect of age and bone mineral density on the absolute, excess, and relative risk of fracture in postmenopausal women aged 50-99: results from the National Osteoporosis Risk Assessment (NORA), Osteoporos Int, 17 (2006) 565-574.

[8] R.B. Martin, D.B. Burr, N.A. Sharkey, Skeletal tissue mechanics, Springer, New York, 1998.

[9] P.R. Cavanagh, A.A. Licata, A.J. Rice, Exercise and pharmacological countermeasures for bone loss during long-duration space flight, Gravit Space Biol Bull, 18 (2005) 39-58.

[10] J. Iwamoto, T. Takeda, Y. Sato, Interventions to prevent bone loss in astronauts during space flight, Keio J Med, 54 (2005) 55-59.

[11] S.M. Smith, M.A. Heer, L.C. Shackelford, J.D. Sibonga, L. Ploutz-Snyder, S.R. Zwart, Benefits for bone from resistance exercise and nutrition in long-duration

spaceflight: evidence from biochemistry and densitometry, J Bone Miner Res, 27 (2012) 1896-1906.

[12] C.M. Bagi, D. Wilkie, K. Georgelos, D. Williams, D. Bertolini, Morphological and structural characteristics of the proximal femur in human and rat, Bone, 21 (1997) 261-267.

[13] R.G. Russell, N.B. Watts, F.H. Ebetino, M.J. Rogers, Mechanisms of action of bisphosphonates: similarities and differences and their potential influence on clinical efficacy, Osteoporos Int, 19 (2008) 733-759.

[14] C. T. Leu, Luegmayr, E., Freedman, L. P., Rodan, G. A., Reszkea, A. A., Relative binding affinities of bisphosphonates for human bone and relationship to antiresorptive efficacy, Bone, 38 (2006) 617-627.

[15] W.S.S. Jee, Cell and tissue biology: a textbook of histology, in: L. Weiss (Ed.), Urban & Schwarzenberg, Baltimore, 1988, pp. xii, 1158 p., 1116 p. of plates.

[16] J.D. Sibonga, Spaceflight-induced bone loss: is there an osteoporosis risk?, Curr Osteoporos Rep, 11 (2013) 92-98.

[17] H.M. Frost, Bone's mechanostat: a 2003 update, Anat Rec A Discov Mol Cell Evol Biol, 275 (2003) 1081-1101.

[18] H.M. Frost, From Wolff's law to the Utah paradigm: insights about bone physiology and its clinical applications, Anat Rec, 262 (2001) 398-419.

[19] M.T. Drake, B.L. Clarke, S. Khosla, Bisphosphonates: mechanism of action and role in clinical practice, Mayo Clin Proc, 83 (2008) 1032-1045.

[20] T.M. Keaveny, W.C. Hayes, A 20-year perspective on the mechanical properties of trabecular bone, J Biomech Eng, 115 (1993) 534-542.

[21] C.H. Turner, Yield behavior of bovine cancellous bone, J Biomech Eng, 111 (1989) 256-260.

[22] T.P. Harrigan, M. Jasty, R.W. Mann, W.H. Harris, Limitations of the continuum assumption in cancellous bone, J Biomech, 21 (1988) 269-275.

[23] R.K. Globus, E. Morey-Holton, Hindlimb unloading: rodent analog for microgravity, J Appl Physiol (1985), 120 (2016) 1196-1206.

[24] Y. Shirazi-Fard, J.S. Kupke, S.A. Bloomfield, H.A. Hogan, Discordant recovery of bone mass and mechanical properties during prolonged recovery from disuse, Bone, 52 (2013) 433-443.

[25] D.N. Kalu, Animal models of the aging skeleton, in: C.J. Rosen, J. Glowacki, J.P. Bilezikian (Eds.), The aging skeleton, Academic Press, San Diego, 1999, pp. xx, 642 p.

[26] P. Sengupta, The laboratory rat: relating its age with human's, Int J Prev Med, 4 (2013) 624-630.

[27] M.F. Delaney, S. Hurwitz, J. Shaw, M.S. LeBoff, Bone density changes with once weekly risedronate in postmenopausal women, J Clin Densitom, 6 (2003) 45-50.

[28] R. Rizzoli, S.L. Greenspan, G. Bone, 3rd, T.J. Schnitzer et al., Two-year results of once-weekly administration of alendronate 70 mg for the treatment of postmenopausal osteoporosis, J Bone Miner Res, 17 (2002) 1988-1996.

[29] M.R. Allen, K. Iwata, R. Phipps, D.B. Burr, Alterations in canine vertebral bone turnover, microdamage accumulation, and biomechanical properties following 1-year treatment with clinical treatment doses of risedronate or alendronate, Bone, 39 (2006) 872-879.

[30] D.M. Reid, D. Hosking, D. Kendler, M.L. Brandi et al., A comparison of the effect of alendronate and risedronate on bone mineral density in postmenopausal women with osteoporosis: 24-month results from FACTS-International, Int J Clin Pract, 62 (2008) 575-584.

[31] S.L. Silverman, N.B. Watts, P.D. Delmas, J.L. Lange, R. Lindsay, Effectiveness of bisphosphonates on nonvertebral and hip fractures in the first year of therapy: the risedronate and alendronate (REAL) cohort study, Osteoporos Int, 18 (2007) 25-34.

[32] A.D. LeBlanc, T.B. Driscol, L.C. Shackelford, H.J. Evans, N.J. Rianon, S.M. Smith, D.L. Feeback, D. Lai, Alendronate as an effective countermeasure to disuse induced bone loss, J Musculoskelet Neuronal Interact, 2 (2002) 335-343.

[33] J.M. Swift, S.N. Swift, M.I. Nilsson, H.A. Hogan, S.D. Bouse, S.A. Bloomfield, Cancellous bone formation response to simulated resistance training during disuse is blunted by concurrent alendronate treatment, J Bone Miner Res, 26 (2011) 2140-2150.

[34] L. Mosekilde, J.S. Thomsen, M.S. Mackey, R.J. Phipps, Treatment with risedronate or alendronate prevents hind-limb immobilization-induced loss of bone density and strength in adult female rats, Bone, 27 (2000) 639-645.

[35] R.K. Fuchs, M. Shea, S.L. Durski, K.M. Winters-Stone, J. Widrick, C.M. Snow, Individual and combined effects of exercise and alendronate on bone mass and strength in ovariectomized rats, Bone, 41 (2007) 290-296.

[36] R.K. Fuchs, R.J. Phipps, D.B. Burr, Recovery of trabecular and cortical bone turnover after discontinuation of risedronate and alendronate therapy in ovariectomized rats, J Bone Miner Res, 23 (2008) 1689-1697.

APPENDIX

A. Additional Figures

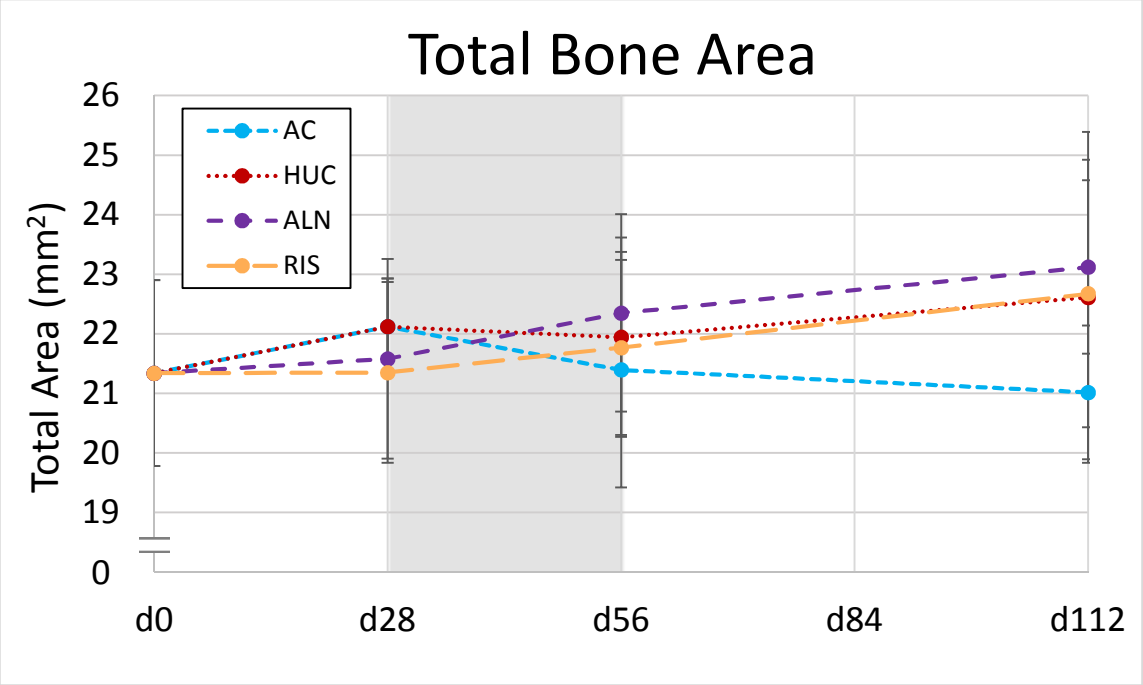

Figure 30: *Ex Vivo* pQCT Total Bone Area of Distal Femur Metaphysis

Hindlimb unloading period is denoted by gray rectangle. Groups not sharing a letter are significantly different from each other. Data are presented as mean ± standard deviation.

There were no significant differences in total bone area at any time point, but n.s. differences at day 112 led to detectable differences in total vBMD not seen in total BMC.

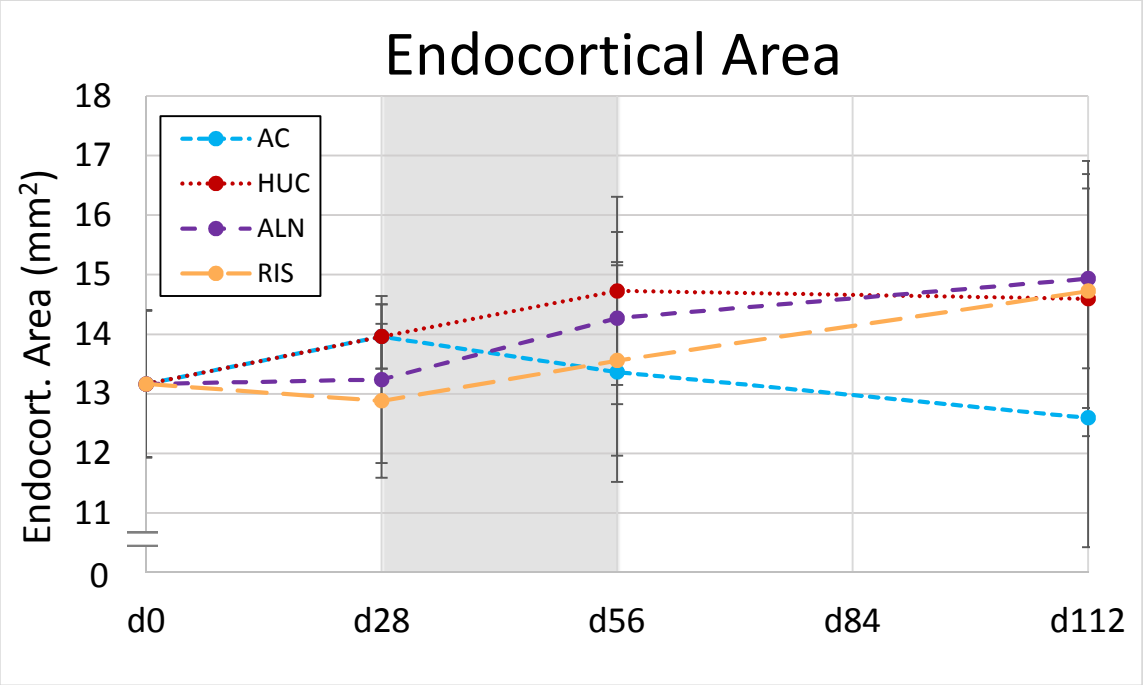

Figure 31: *Ex Vivo* pQCT Endocortical Area of Distal Femur Metaphysis

Hindlimb unloading period is denoted by gray rectangle. Groups not sharing a letter are significantly different from each other. Data are presented as mean ± standard deviation.

No significant differences at any time point with the greatest spread occurring at day 112. The n.s. difference between HUC and AC at day 56 led to a detectable significant difference between the groups in cancellous vBMD that was not seen in cancellous BMC. At day 112, the n.s. difference between ALN and AC accounted for the significant difference in BMC and thus vBMD for those groups did not differ.

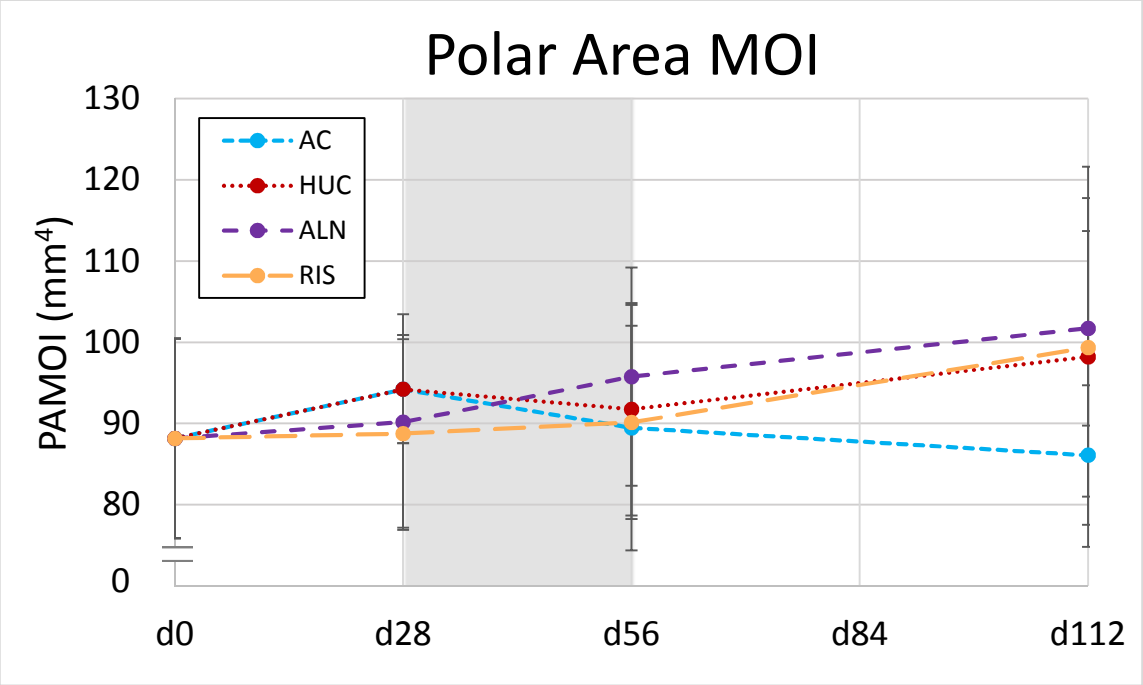

Figure 32: *Ex Vivo* pQCT Polar Area Moment of Inertia of Distal Femur Metaphysis

Hindlimb unloading period is denoted by gray rectangle. Groups not sharing a letter are significantly different from each other. Data are presented as mean ± standard deviation.

There were no significant differences in PAMOI at any time point and there was high variability with higher spread of group averages.

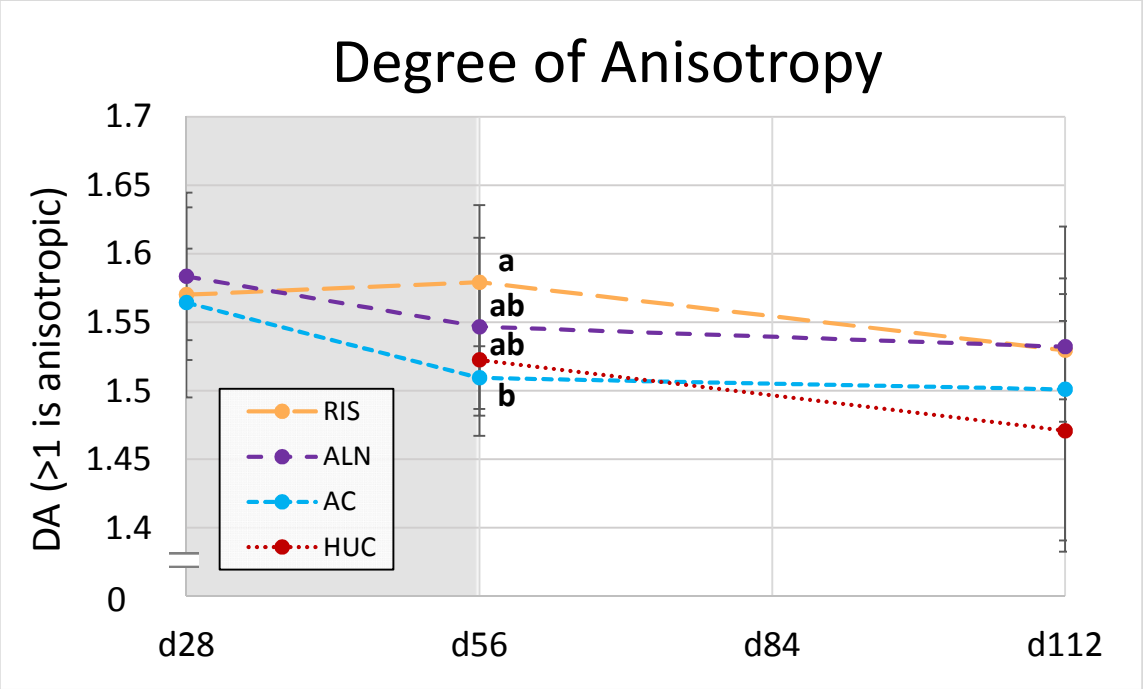

Figure 33: *Ex Vivo* µCT Degree of Anisotropy of Distal Femur Metaphysis

Hindlimb unloading period is denoted by gray rectangle. Groups not sharing a letter are significantly different from each other. Data are presented as mean ± standard deviation.

At day 56, the DA is significantly lower for the AC group compared to the RIS group. This difference is small but the fact that both treatment groups either trend higher or are significantly higher than both controls is interesting. That would suggest that BP-treated bone is somewhat more directionally dependent on a whole. There were no between-group differences at day 112.